Calculation of Disruption Halo Currents and Forces with the M3D Code

J. A. Breslau

Workshop on Theory and Simulation of Disruptions

Princeton, NJ

July 9, 2014

Outline

- Review of NSTX VDE validation study
  - Experimental observations
  - M3D results
- The challenge to the M3D model
- Verification with the Zakharov test problem
  - Equilibrium
  - Linear stability
  - Nonlinear saturation of free boundary kink
  - Nonlinear saturation of wall-touching kink
- Conclusions

Why VDEs?

- Spontaneous failure of the feedback system providing vertical stability control is *not* a common cause of disruptions…

- …however, many *other* failure modes for tokamak confinement eventually result in loss of vertical control, particularly if they are not detected in time for an emergency shutdown…

- …and the contact of the plasma with the vacuum vessel in a VDE results in large halo currents that result in high transient forces…

- …so VDEs are logical to study when designing a device to handle worst-case-scenario events.

NSTX XP833 (2010):

Halo current dependencies on I_p/q_{95}, vertical velocity, and halo resistance

Reference shot without forced disruption drive, based on 129416:

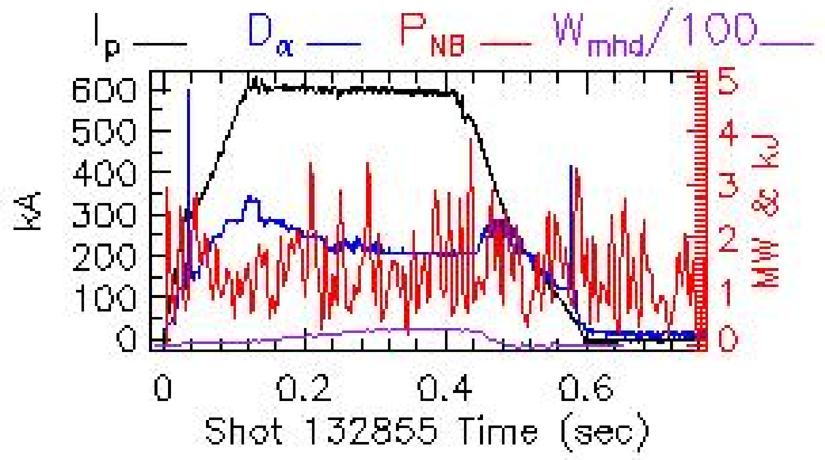

Shot 132859, with deliberately misadjusted vertical field control, terminates in VDE:

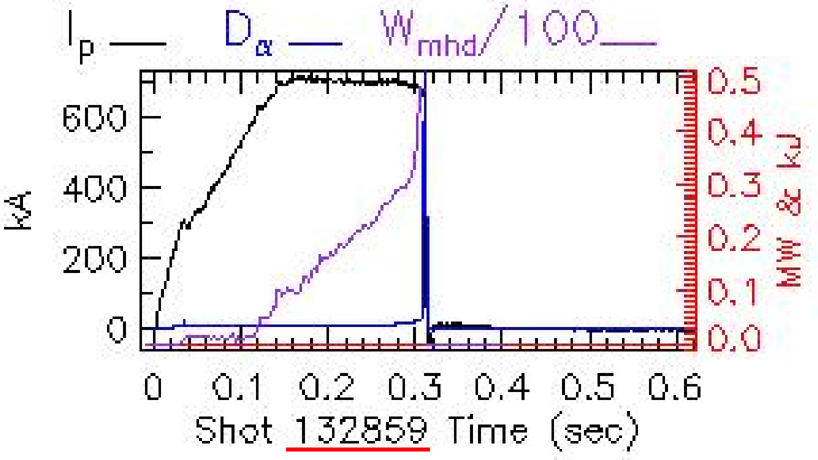

S. Gerhardt

Layout of NSTX halo current diagnostics

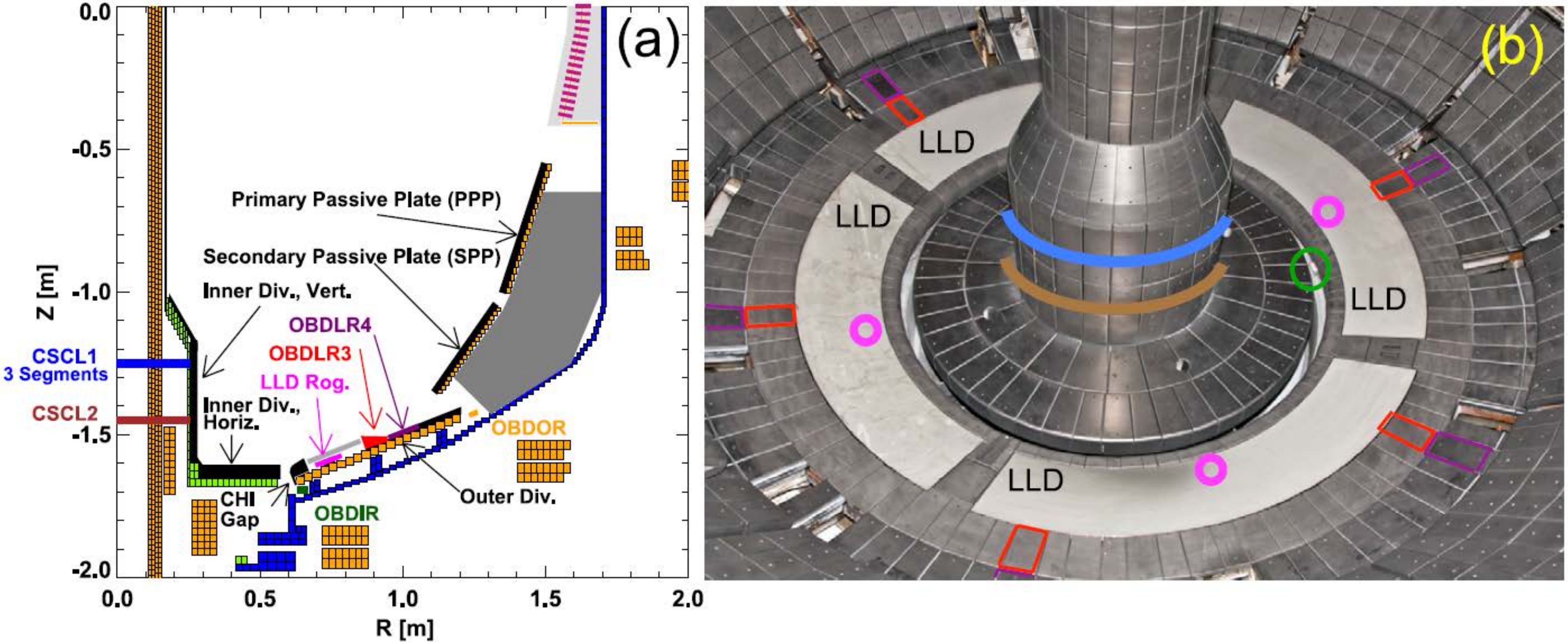

Halo current is inferred from transient TF measurements under several divertor tiles and plates at about six toroidal locations. Transient vessel forces are not measured.

Figure reproduced from S.P. Gerhardt, J. Menard, S. Sabbagh and F. Scotti, *Nucl. Fusion* **52** (2012).

Strongly Non-Axisymmetric Halo Currents Detected in the NSTX Lower Divertor

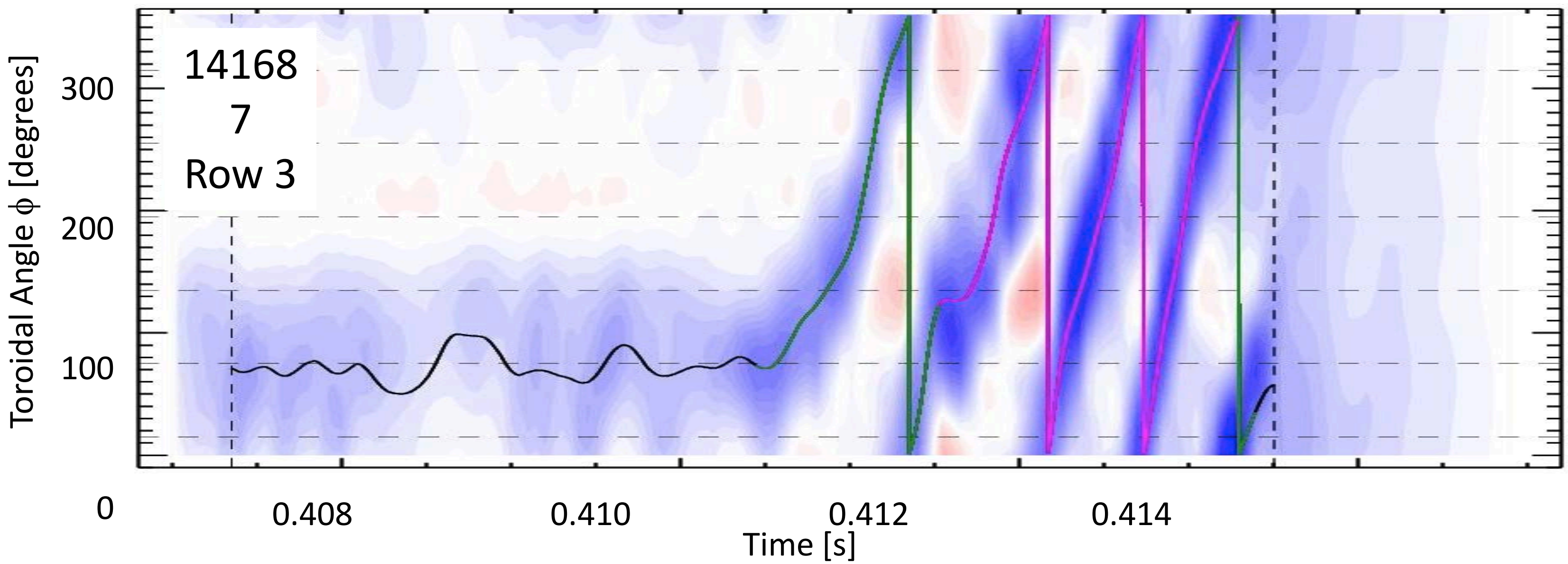

- Infer strong toroidal asymmetry, often with significant rotation, at locations where currents enter the divertor floor.

<u>Key Observations</u>

Dominant structure is typically a toroidally-rotating lobe.
Rotation is typically in the counter-direction, except for short bursts.

S. Gerhardt

Meshing the NSTX Vessel for Simulation

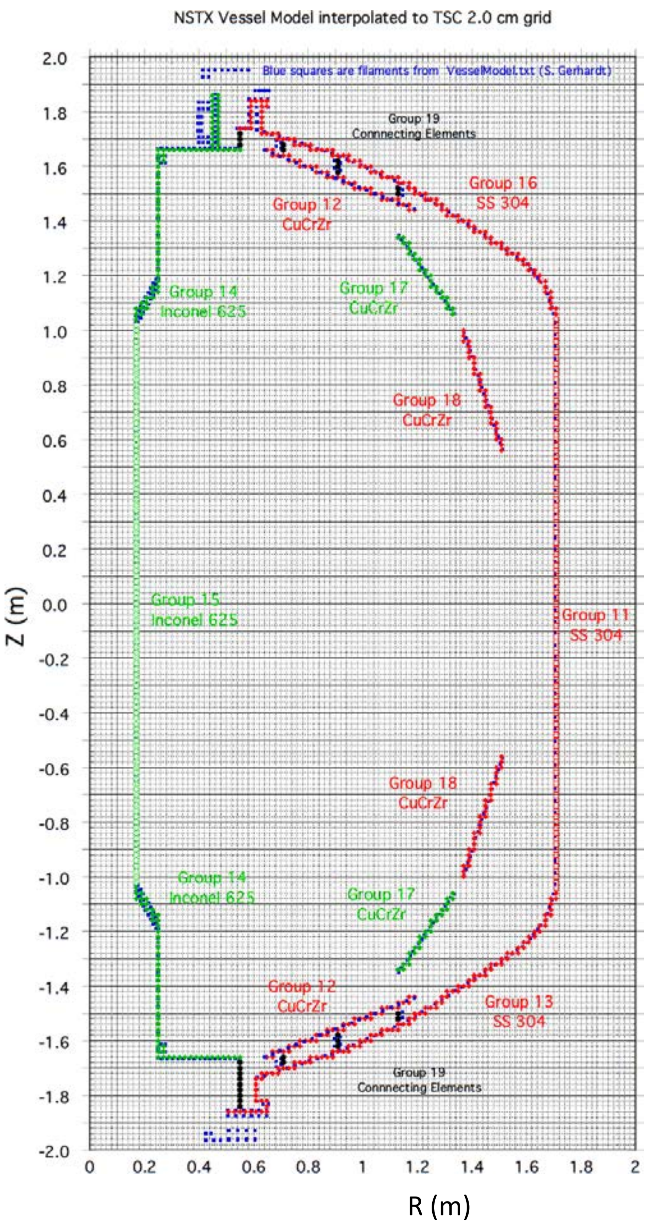

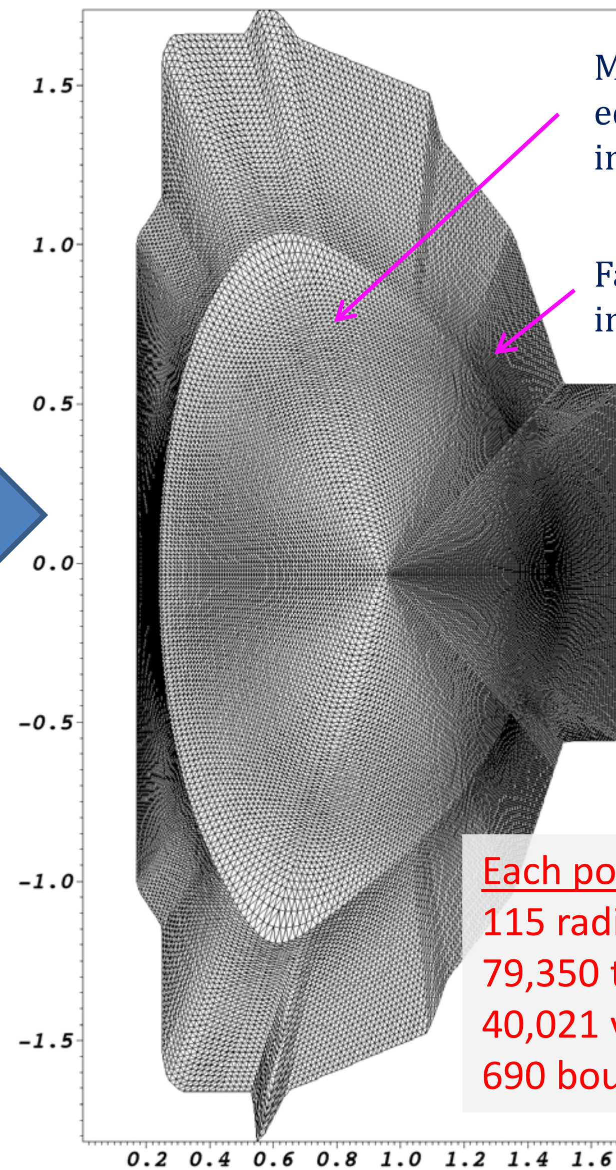

Mesh aligned to equilibrium flux surfaces inside separatrix

Fairly uniform spacing in vacuum region

Thin, axisymmetric uniformly resistive shell

Each poloidal section has up to
115 radial zones
79,350 triangular elements
40,021 vertices
690 boundary vertices

n=1 eigenmode

η_0	5×10^{-8}
η_{vac}	1.67×10^{-4}
η_{wall}	0
μ_0	5×10^{-7}
μ_{edge}	10^{-4}
$\kappa_\perp$	10^{-5}
$\kappa_{\|\|}$	10^{-1}

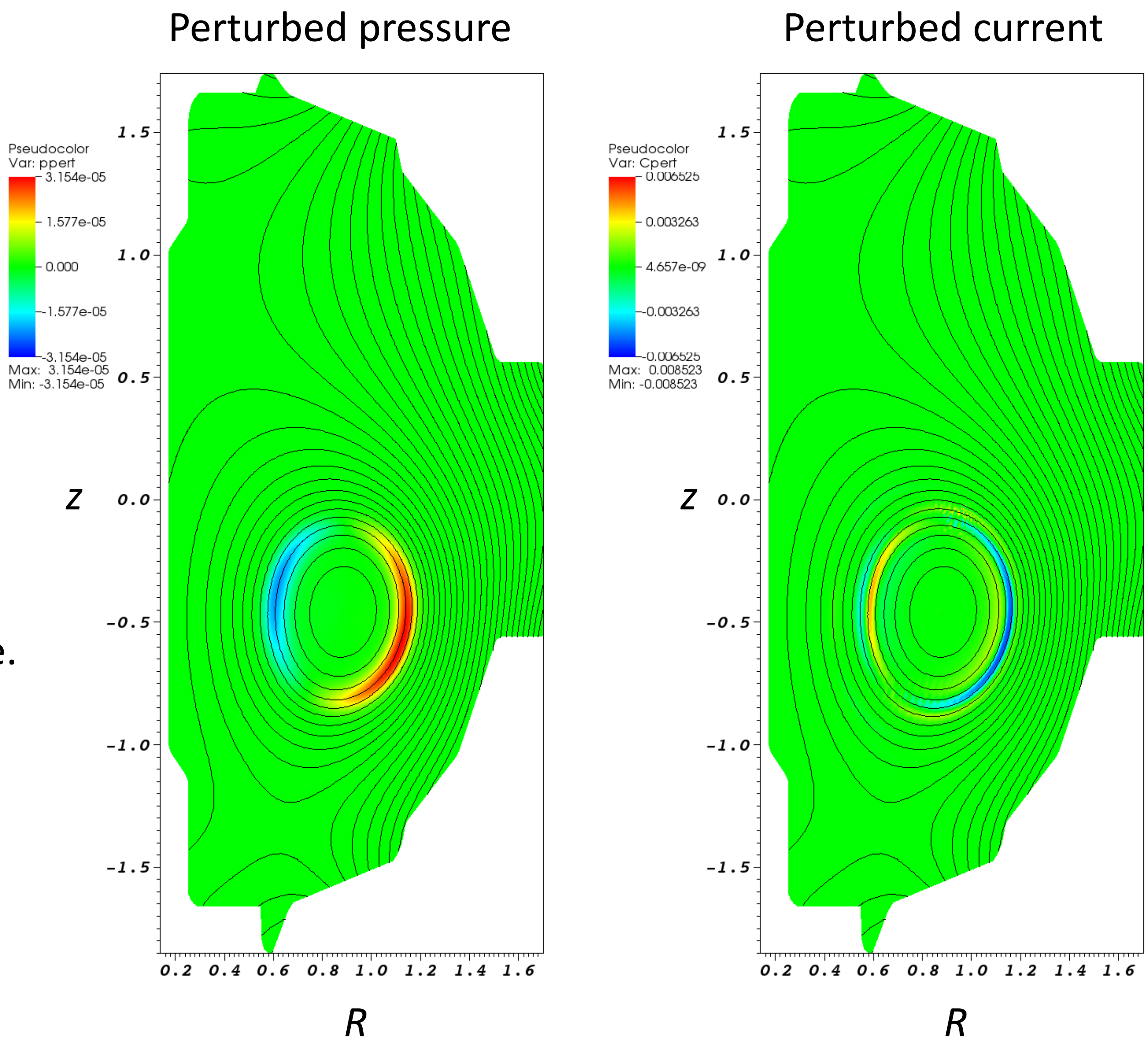

Predominantly 1,1 mode at q=1 surface.

$\gamma \approx 6.5 \times 10^{-2}$

Snapshots of Nonlinear Evolution

t = 177.14

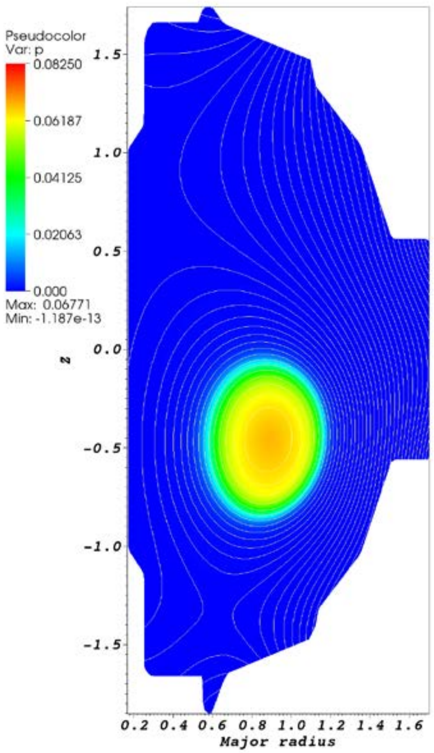

Ideally unstable displaced plasma

t = 222.99

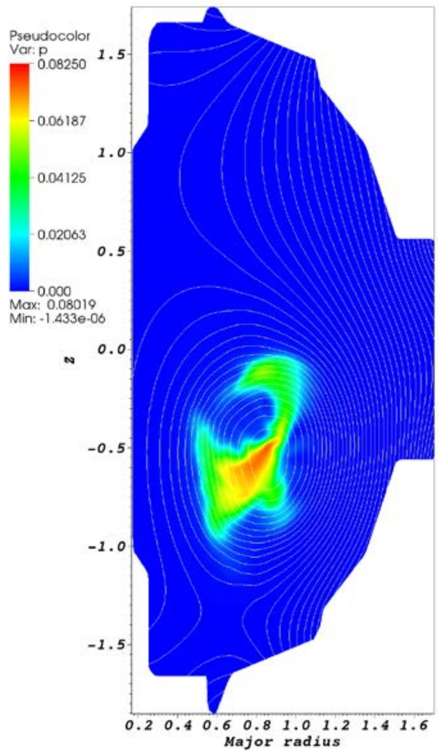

Instability couples many toroidal & poloidal modes…

t = 284.15

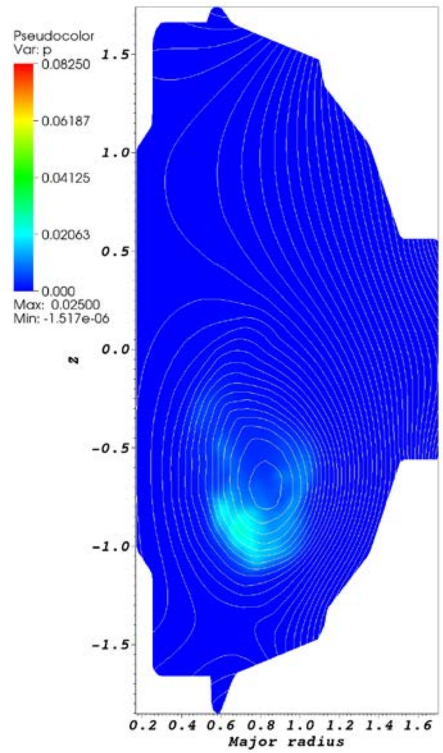

…leading to rapid thermal quench.

t = 361.49

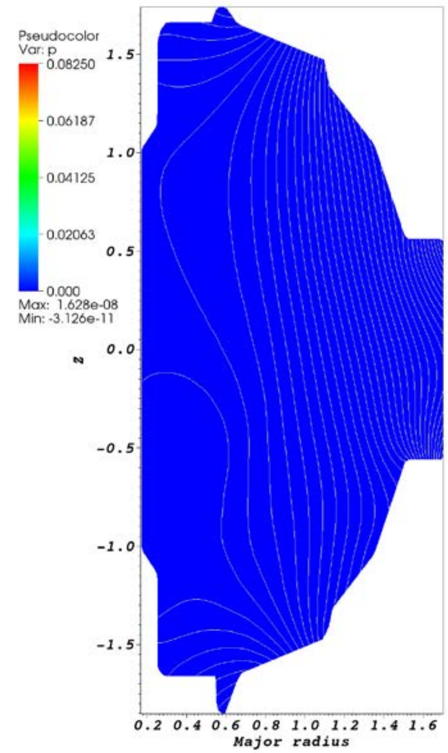

Current quench follows.

Time History (nonlinear 3D phase)

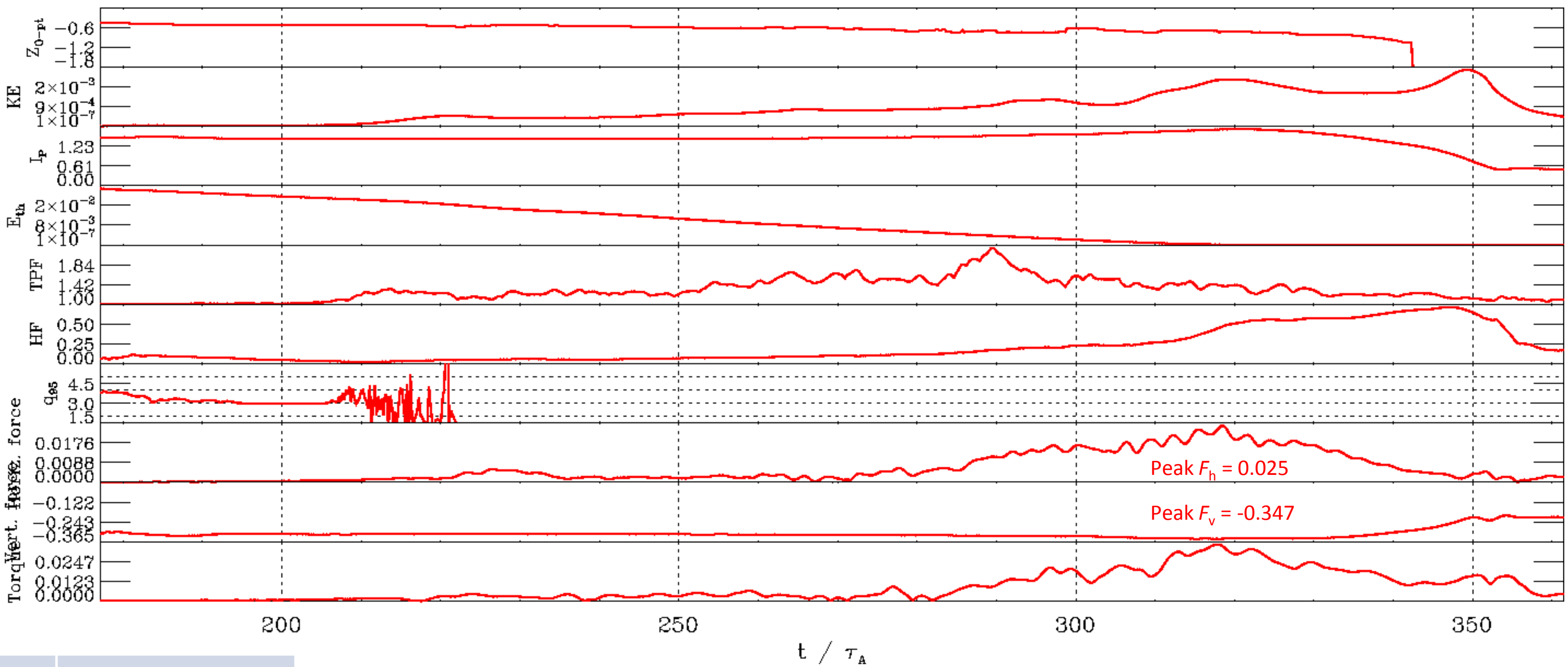

η_0	5×10^{-8}
η_{vac}	1.67×10^{-4}
η_{wall}	10^{-4}
μ_0	5×10^{-7}
μ_{edge}	10^{-4}
$\kappa_\perp$	10^{-5}
$\kappa_{\|\|}$	10^{-1}

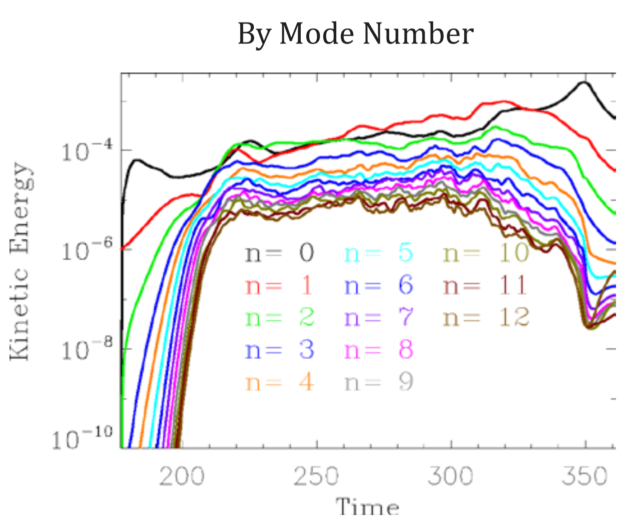

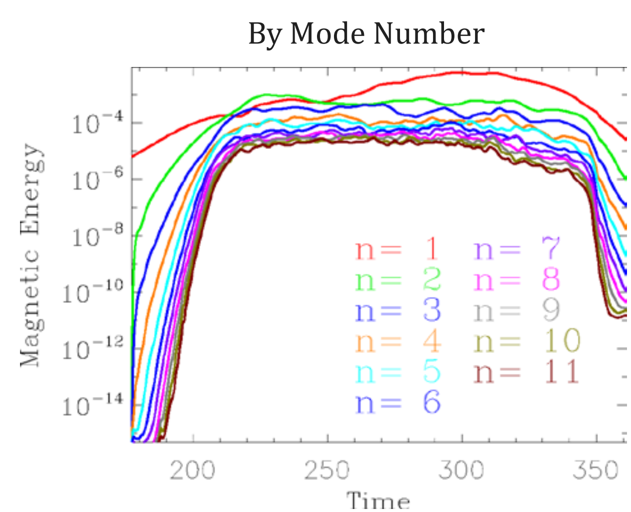

Halo Current Distribution at Peak

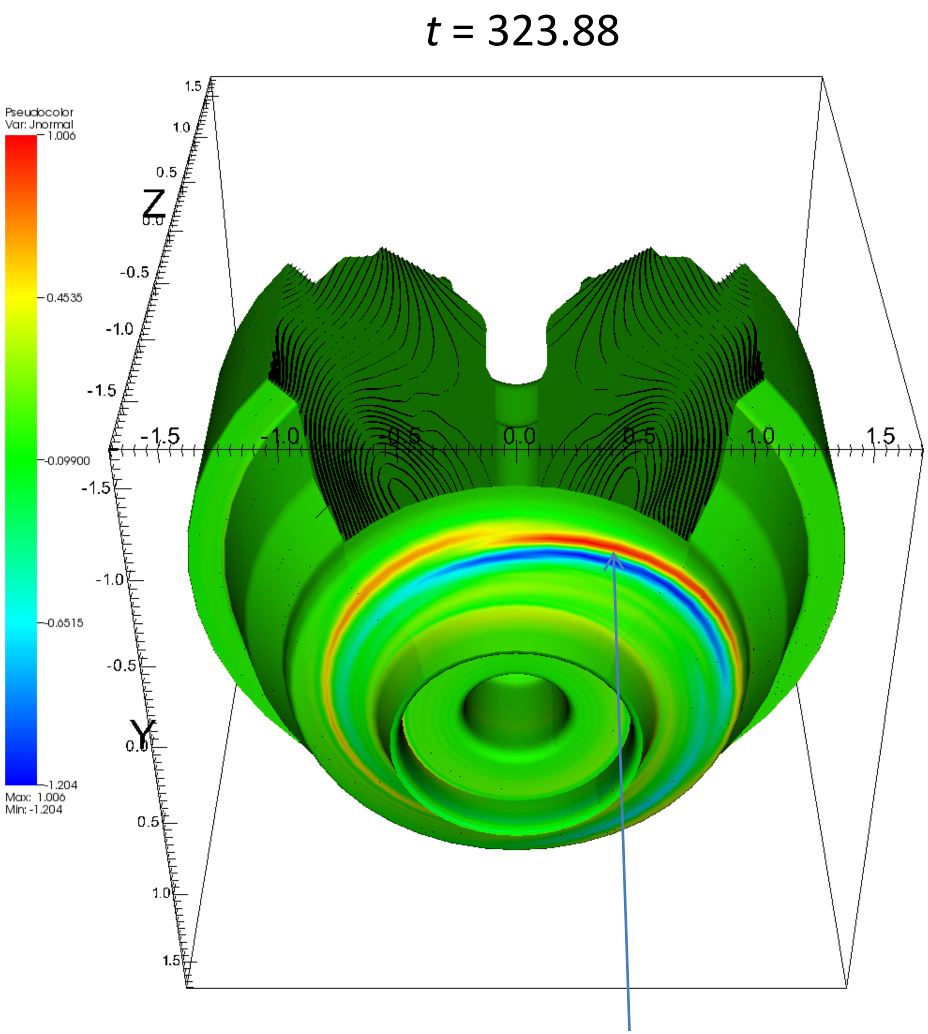

Current peaks on lower Group 12 plate.

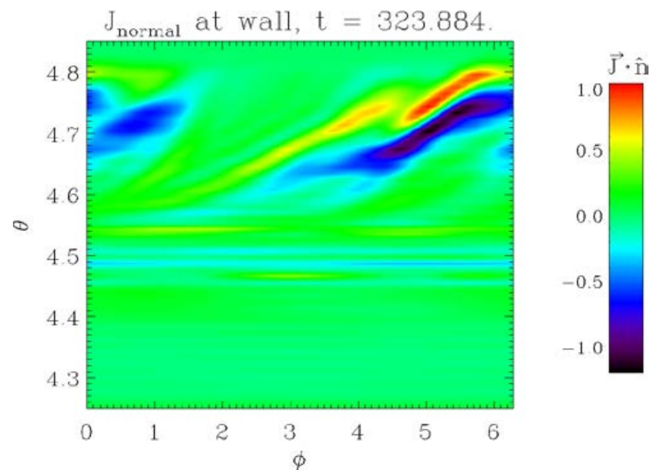

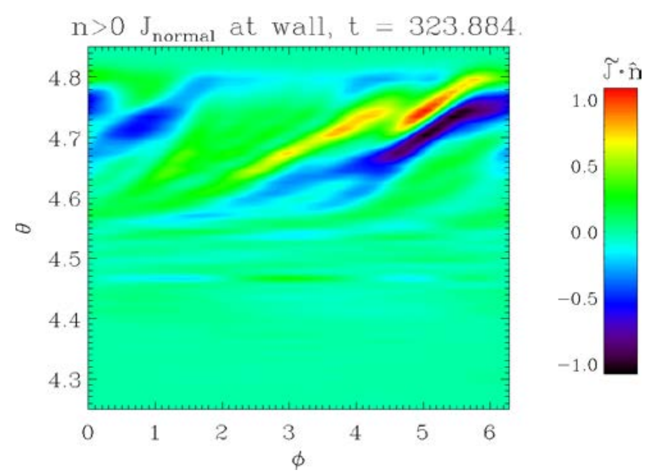

n=1 component strongly dominates over *n*=0.

Halo Current Distribution vs. Time

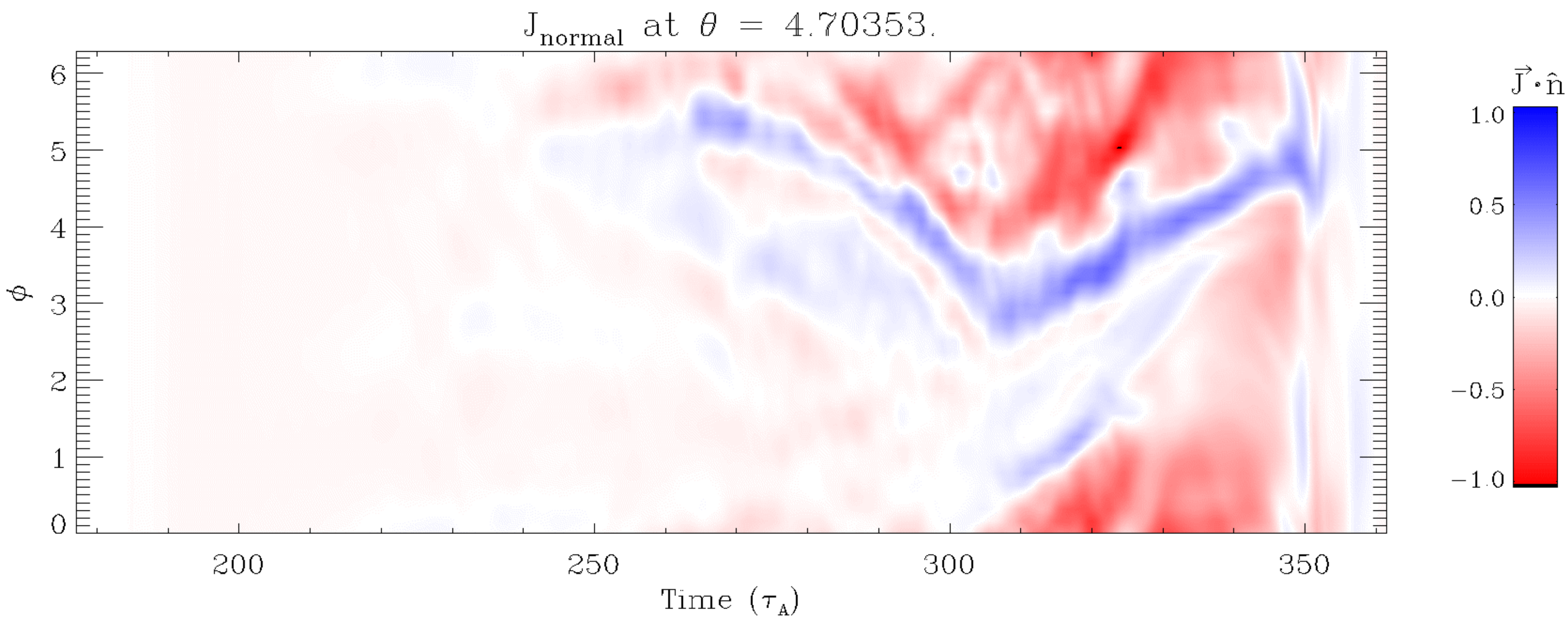

Validation Conclusions

- MHD simulation plausibly accounts for most observed qualitative features of NSTX VDEs, including degree of toroidal peaking.

- The largest transient horizontal vessel forces occur when $\gamma\tau_w \sim 1$; this can be generalized to other devices.

- High TPF can still occur for large τ_w if the plasma is already significantly displaced when the ideal n=1 mode is triggered.

- Peak horizontal force is an order of magnitude lower than vertical force in NSTX; this may not apply to other devices.

Controversy

- The reliability of these results has been challenged on the basis of the code's "saltwater" boundary conditions: unlike in the actual system, the normal velocity of the plasma in the model is constrained to vanish at the boundary.

- Put this to the test by applying the M3D model to a simplified test case devised and run by the issuer of the challenge, and comparing the numerical results.

The Zakharov Test Problem

- Straight cylinder equilibrium, circular cross-section
  - Plasma minor radius at r=0.6, tile surface at r=0.7, ideal wall at r=1.0.
  - Tile surface behaves as a perfect insulator before plasma reaches it; perfect conductor thereafter.
  - Plasma interior $q \equiv 1.0$; edge q=0.75.
  - Plasma pressure low, flat; conductivity infinite.

- Evolve 1,1 external kink mode with 2D version of Disruption Simulation Code (**DSC**) called Cbwtk.
  - Implements Kadomtsev-Pogutse single helicity MHD model.
  - Eliminates inertia by replacing the momentum equation with

$$\rho \frac{d\mathbf{V}}{dt} \rightarrow \gamma \mathbf{V} = \lambda \vec{\xi}$$

DSC Results

Free boundary kink (FBK) with ideal wall

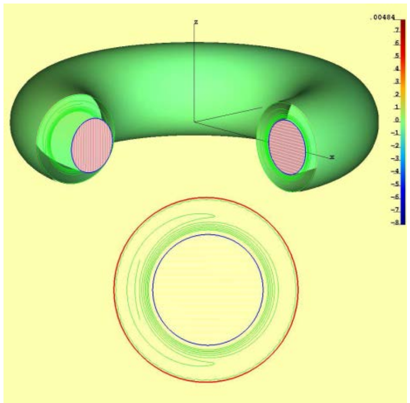

Initial perturbed plasma

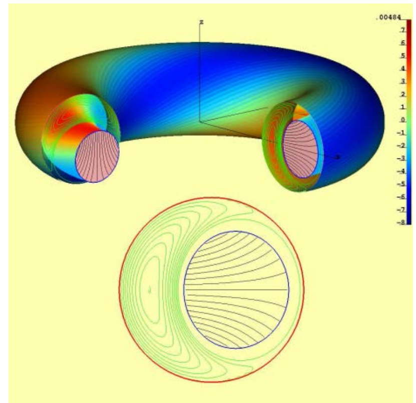

Fast phase of instability

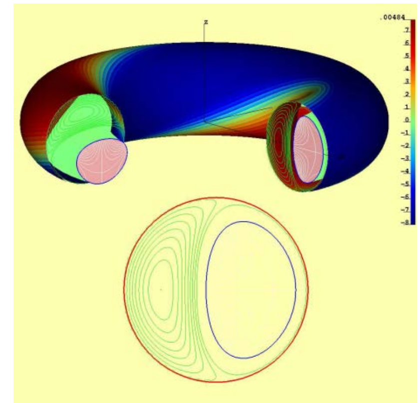

Saturation of the mode

Wall-touching kink (WTK) at tile surface

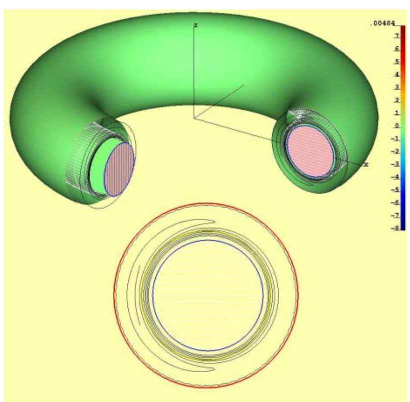

Initial perturbed plasma

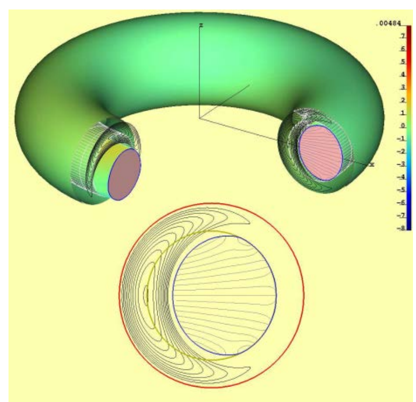

Fast phase of instability, excitation of Hiro currents

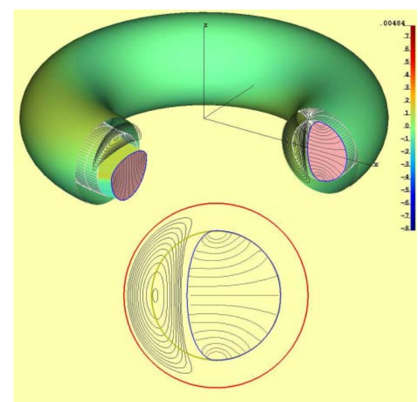

Saturation of the mode due to Hiro currents

The M3D Code

M3D (multi-level 3D) is a parallel 3D nonlinear initial-value extended MHD code in toroidal geometry maintained by a multi-institutional collaboration.

- Physics models include ideal and resistive MHD; two-fluid with just ω* or ω* and Hall terms; or hybrid with kinetic hot ions or kinetic bulk ions and fluid electrons.
- Uses linear, C^0 triangular finite elements on an unstructured mesh in-plane.
- Uses 4^{th}-order finite differences between planes or pseudo-spectral derivatives.
- Partially implicit treatment allows efficient advance over dissipative and fast wave time scales but requires small time steps relative to τ_A.
- Halo and vacuum regions are modeled as low-temperature plasmas, with $\eta \propto T^{-3/2}$ and heat rapidly conducted to the cold wall along open field lines.

Resistive MHD Equations

$$\frac{\partial \rho}{\partial t} + \nabla \cdot \left(\rho \mathbf{v} \right) = 0$$

$$\rho \left(\frac{\partial \mathbf{v}}{\partial t} + \mathbf{v} \cdot \nabla \mathbf{v} \right) = -\nabla \mathbf{p} + \mathbf{J} \times \mathbf{B} + \mu \nabla^2 \mathbf{v}$$

$$\mathbf{E} + \mathbf{v} \times \mathbf{B} = \eta \mathbf{J}$$

$$\frac{\partial \mathbf{B}}{\partial t} = -\nabla \times \mathbf{E}$$

$$\mathbf{J} = \nabla \times \mathbf{B}$$

$$\frac{\partial p}{\partial t} + \mathbf{v} \cdot \nabla p = -\gamma p \nabla \cdot \mathbf{v} + \nabla \cdot \left\{ n \left[\chi_{||} \nabla_{||} \left(\frac{p}{\rho} \right) + \chi_{\perp} \nabla_{\perp} \left(\frac{p}{\rho} \right) \right] \right\}$$

Approximation used for M3D equilibrium

- Large-aspect-ratio torus, circular cross-section.
- In plasma ($0 \le r \le a$-δ), constant *p* and *q* provided by :

$$RB_\phi(r) = \frac{q_0^2 R_0^2 B_0}{q_0^2 R_0^2 + r^2} \qquad J_\phi(r) = \frac{2 q_0^3 R_0^3 B_0}{\left(q_0^2 R_0^2 + r^2\right)^2} \qquad p(r) = p_0$$

- In boundary layer (a-$\delta \le r \le a$) $q \to q_a$, *p* drops linearly:

$$RB_\phi(r) = \frac{q_0^2 R_0^2 B_0}{q_0^2 R_0^2 + (a-\delta)^2} \qquad J_\phi(r) = \frac{\gamma r}{\sqrt{\dfrac{2\gamma\left(r^3 - a^3\right)}{3} + \dfrac{a^4 B_{b,z}^2}{q_a^2 R_0^2}}} \qquad p(r) = p_0 - \gamma\left[r - (a-\delta)\right]$$

- In vacuum, *p* is low, *J* vanishes, fields are continuous:

$$RB_\phi(r) = \frac{q_0^2 R_0^2 B_0}{q_0^2 R_0^2 + (a-\delta)^2} \qquad J_\phi(r) = 0 \qquad p(r) = \varepsilon$$

- Here, q_0=B_0=1, q_a=0.75, a=0.6; the aspect ratio R_0, layer thickness δ, and pressure ratio p_0/ε are free parameters, and

$$\gamma = \frac{3}{2\left[(a-\delta)^3 - a^3\right]}\left\{\frac{q_0^2 R_0^2 B_0^2 (a-\delta)^4}{\left[q_0^2 R_0^2 + (a-\delta)^2\right]^2} - \frac{a^4 B_{b,z}^2}{q_a^2 R_0^2}\right\}, \quad p_0 = \varepsilon + \gamma\delta$$

Equilibrium Relaxation

- R_0=18, δ/a=0.1, p_0/ε=100, n_0/n_{vac}=1 $\rightarrow$ T_0/T_{vac} = 100
- 190 radial zones

pressure

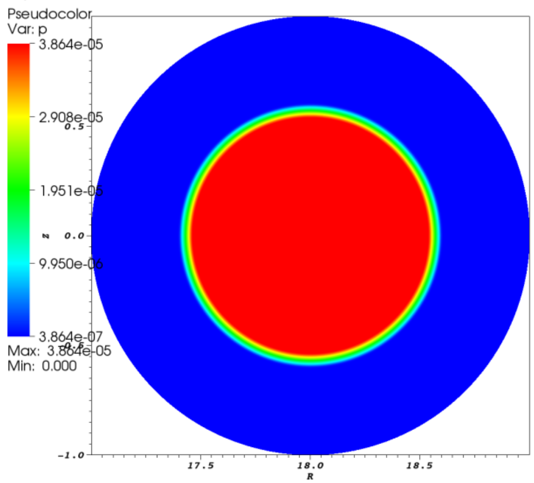

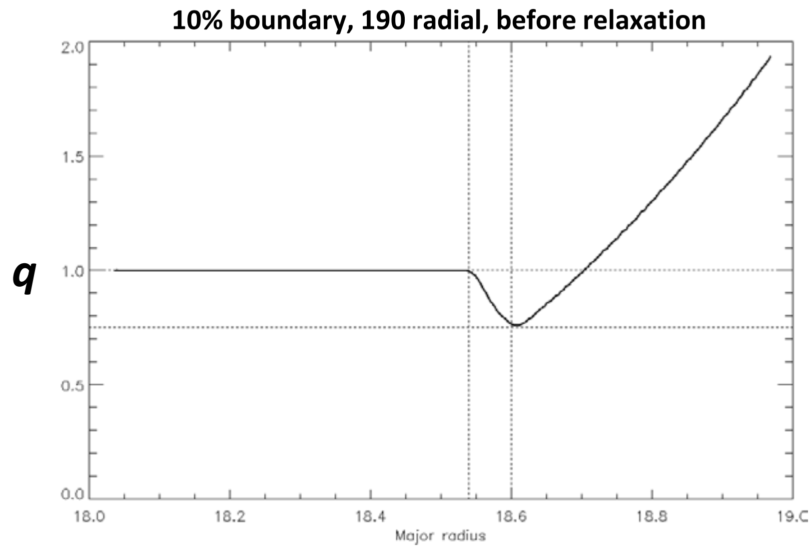

toroidal current density

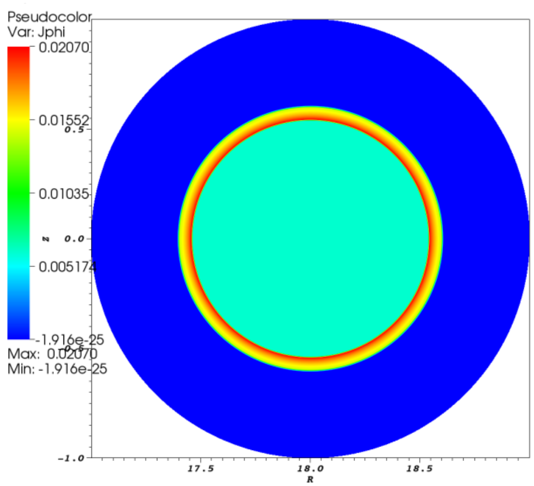

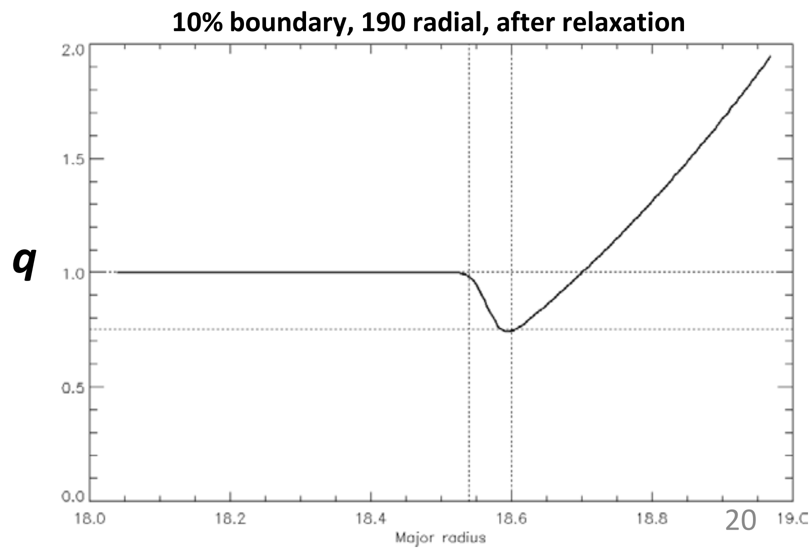

Current sheet resolution (detail)

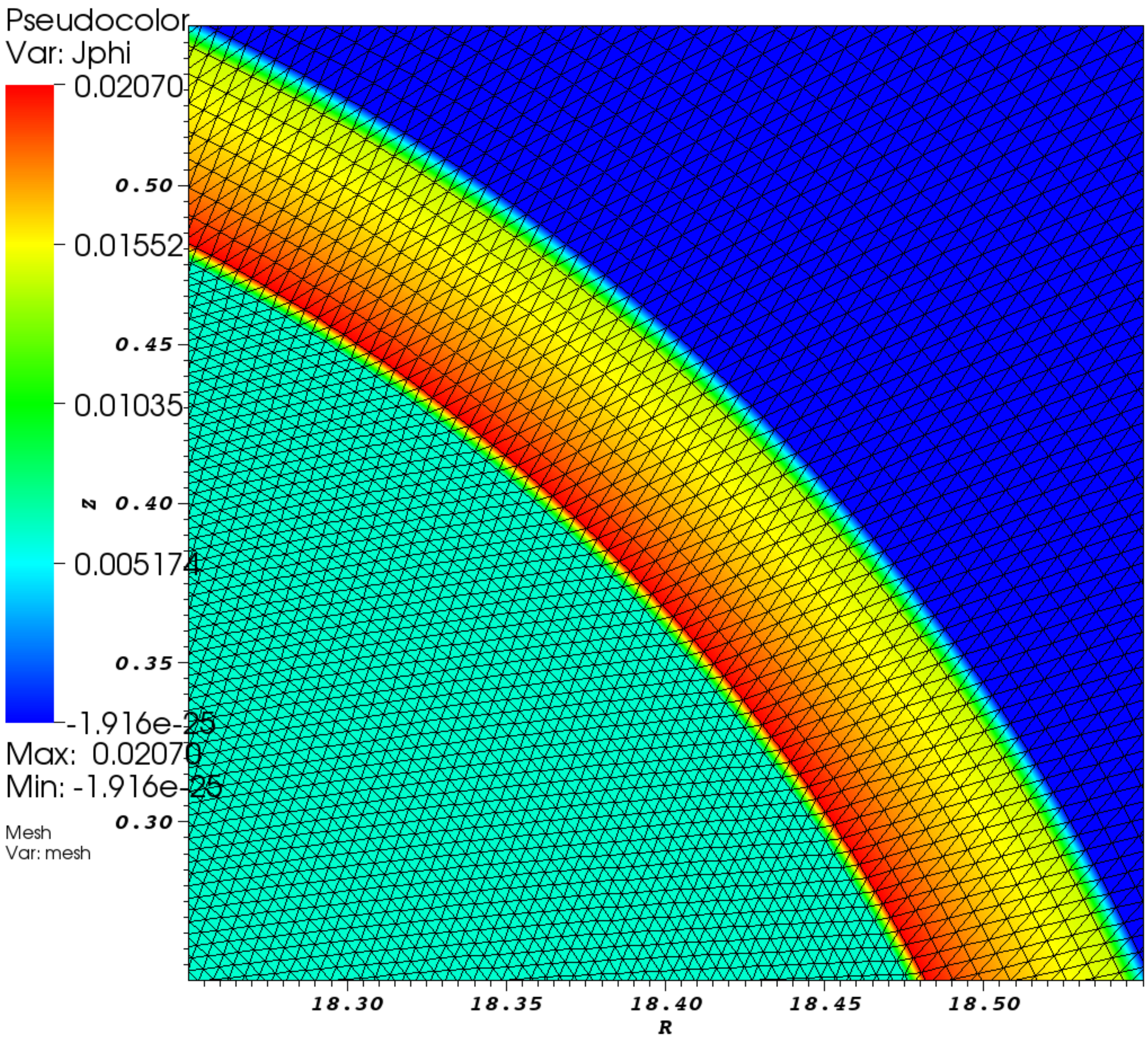

The kink perturbation

- Zakharov's perturbation is a small helical deformation of the plasma surface:

$$\rho \to a + \xi_{1,1} \cos(\omega - \phi)$$

- This is a rigid rightward displacement of the plasma column.

- M3D perturbs the incompressible poloidal velocity stream function to achieve the same effect:

$$U_0(r,\theta,\phi) = \begin{cases} r\xi_{1,1} \sin(\theta - \phi), & 0 \le r \le a \\ 0, & a < r \end{cases}$$

- Run linearly to find eigenmode, then use it as small initial perturbation for 3D nonlinear calculation.

Linear eigenmode calculation

Initial perturbation

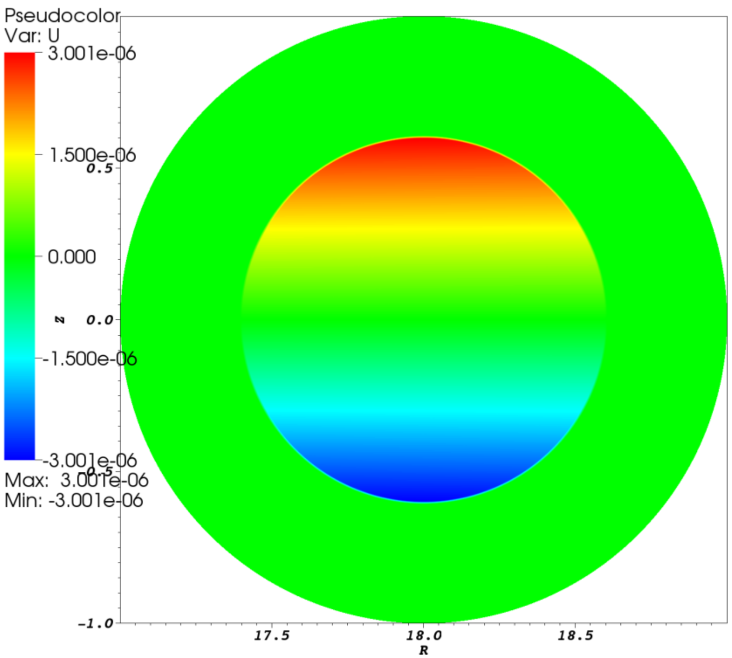

n=1 eigenmode
is a 1,1 external kink

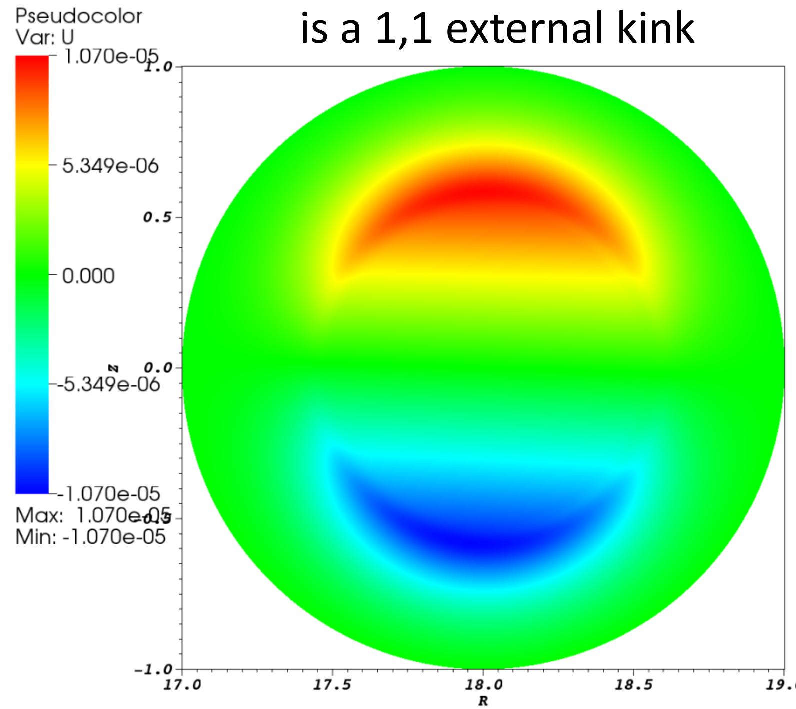

Details:

$\eta_{plas} = 10^{-6}$; $\eta_{vac} \approx 9.5 \times 10^{-4}$; $\eta_{\rm wall} = 0$

$\mu = 10^{-5}$; $\mu_{\rm H\_tor} = 10^{-3}$

$\kappa_{\perp} = 10^{-6}$; $\kappa_{||} = 5 \times 10^{2}$

density evolution off

ohmic heating on

$\gamma\tau_A = 0.0210 \pm 0.00105$

Eigenmode current and flow patterns

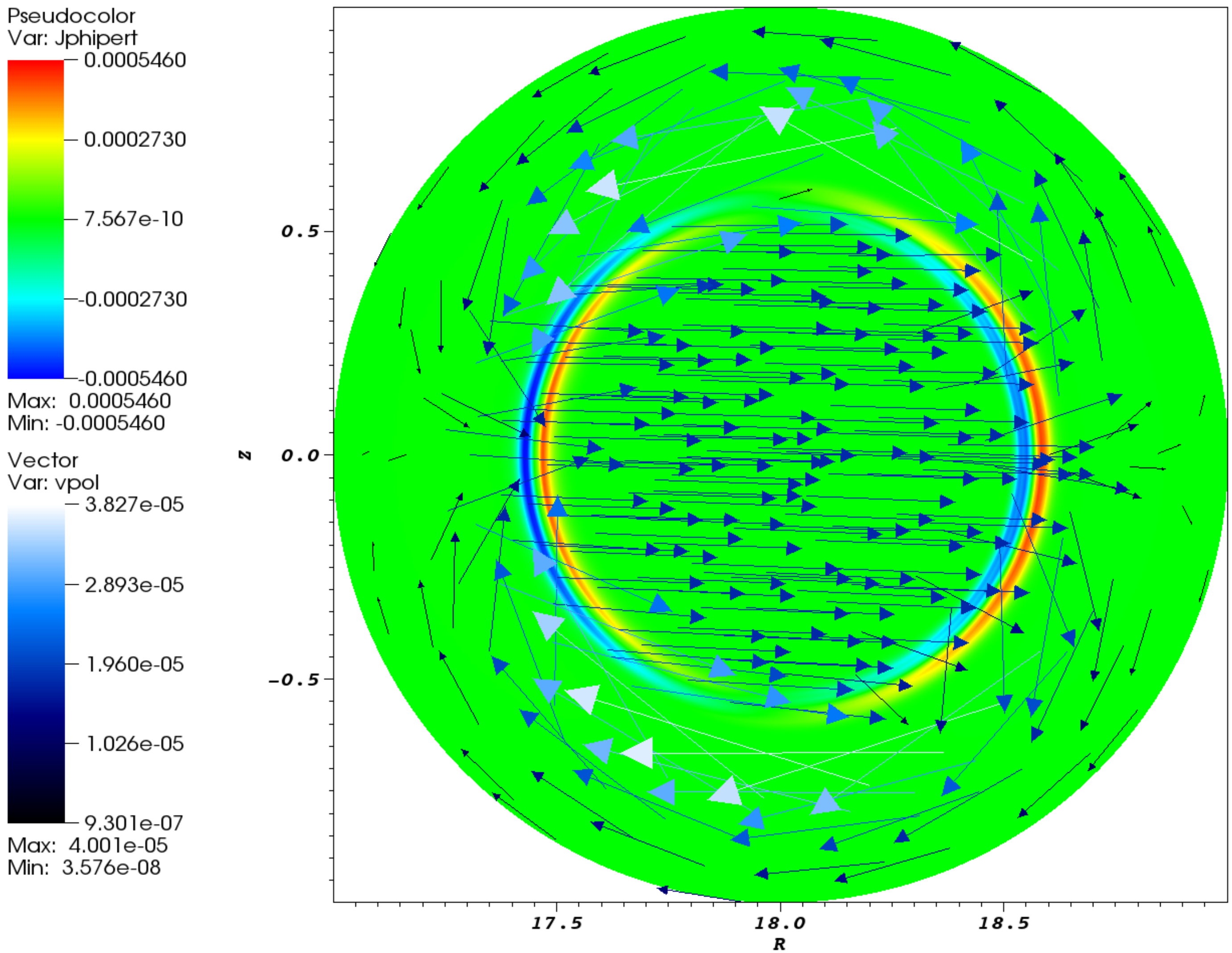

- Rigid displacement of plasma column
- Rearrangement of “vacuum” to avoid compression
- 1,1 toroidal current sheets of both signs at plasma boundary

Higher *n* modes are also unstable

n=2 eigenmode

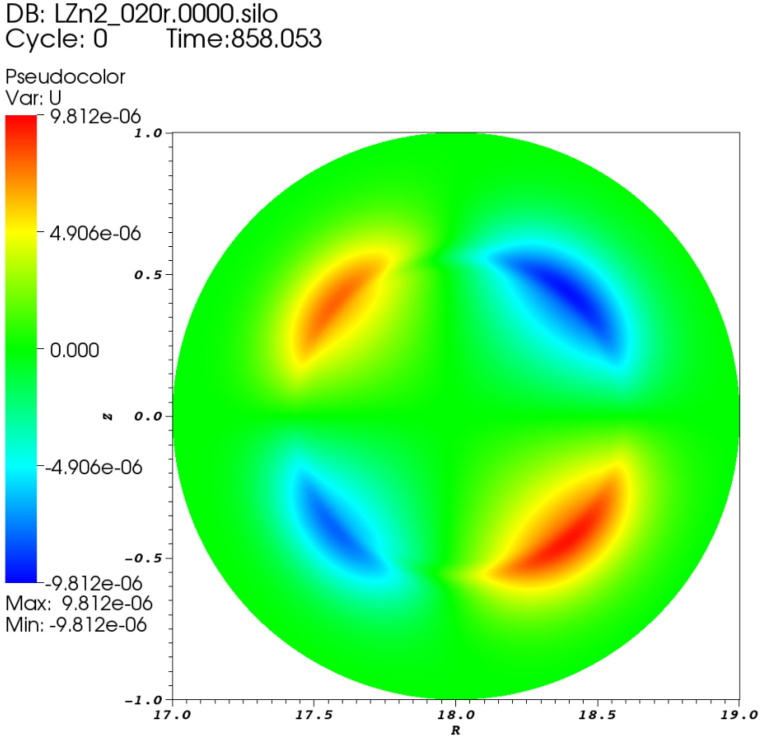

$\gamma\tau_A = 0.0265 \pm 0.0005$

n=3 eigenmode

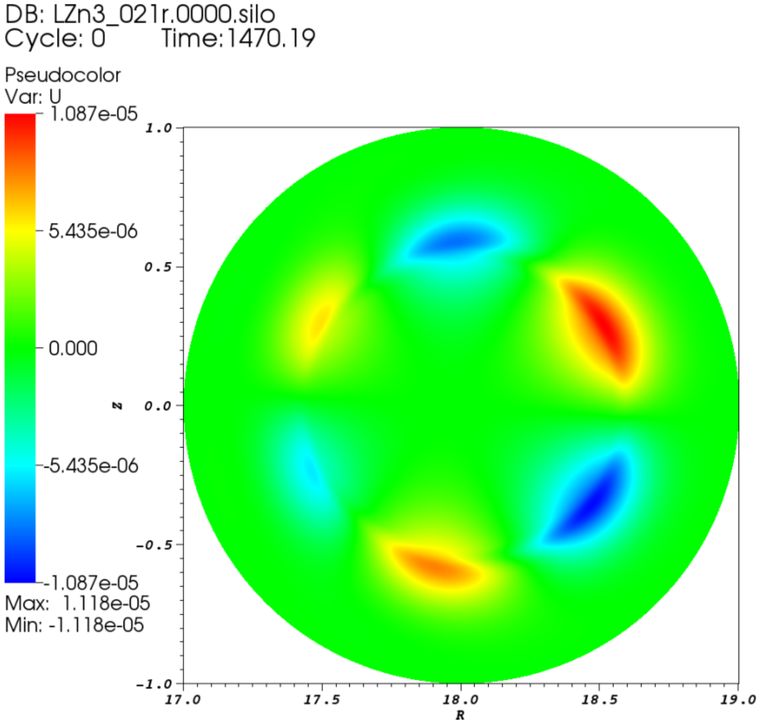

$\gamma\tau_A = 0.01415 \pm 0.0012$

Full 3D nonlinear behavior, ideal wall only (FBK)

Details:

$\eta_{plas} = 10^{-6}$; $\eta_{vac} \approx 9.5 \times 10^{-4}$; $\eta_{\mathrm{wall}} = 0$

$\mu = 10^{-5}$; $\mu_{\mathrm{H\_tor}} = 10^{-3}$

$\kappa_{\perp} = 10^{-6}$; $\kappa_{||} = 5 \times 10^{2}$

initial pert.: n=1 only

density evolution off

ohmic heating on

$0 \leq n \leq 9$ (32 planes)

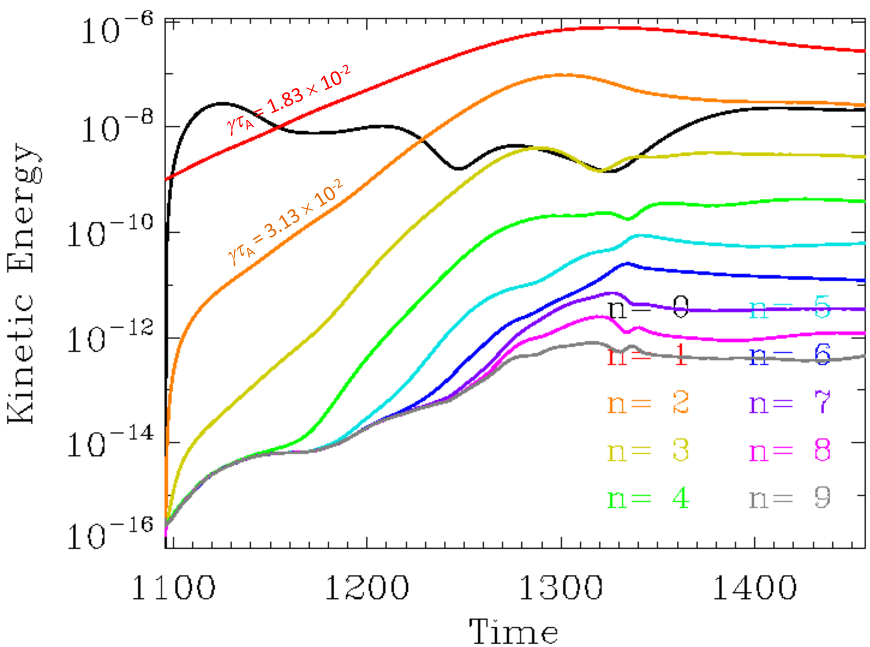

n=1 KE saturates at 7.703×10^{-7} in 229 Alfvén times.

Approx. plasma boundary vs. time

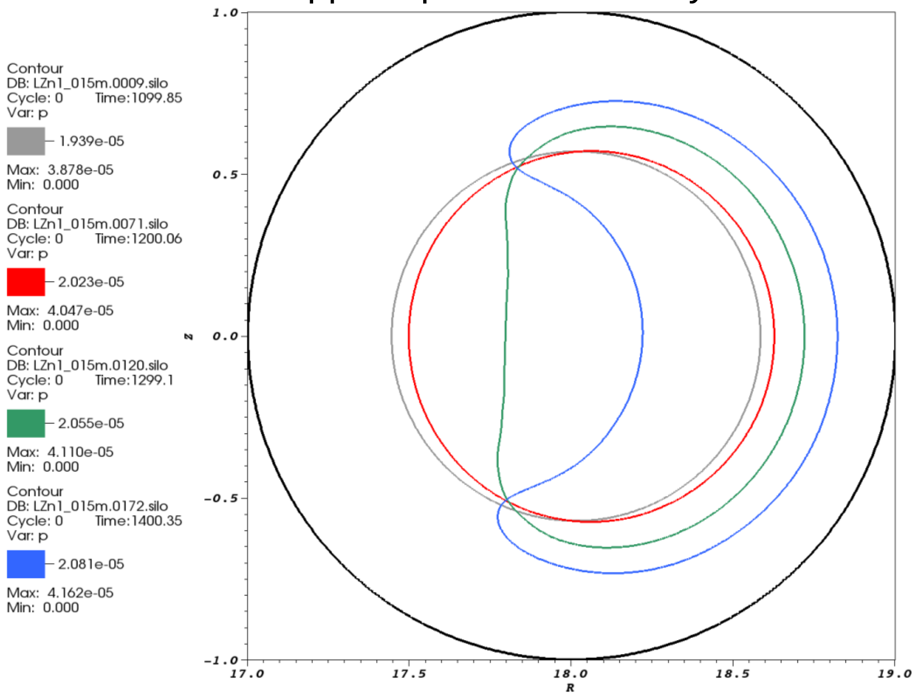

D-shape gives way to crescent as vacuum bubble penetrates plasma column.

FBK Plasma currents during D phase

(t = 1281.06)

Total toroidal current density, ϕ=0

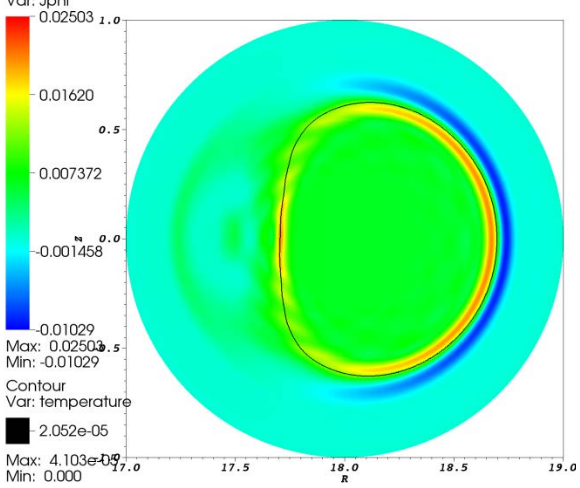

n>0 toroidal current density, ϕ=0

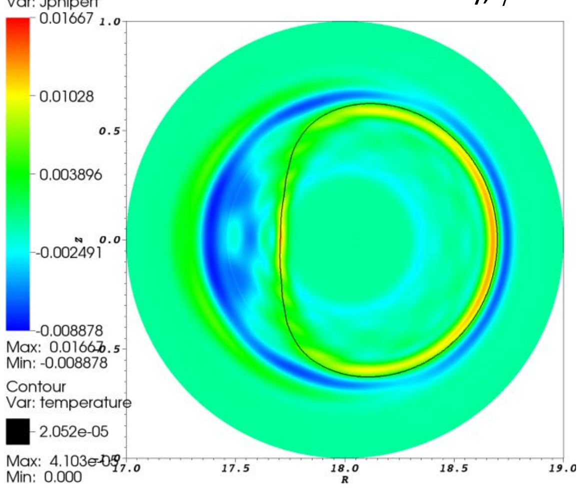

n>0 toroidal current density
on transformed T=2.05×10^{-5} surface

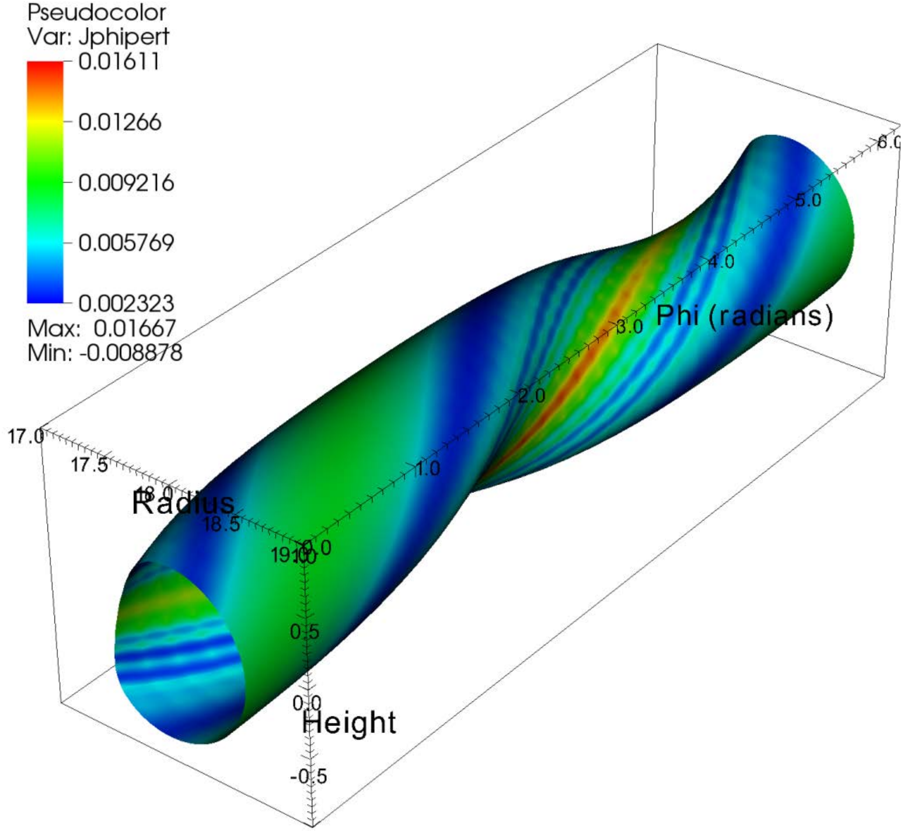

FBK Plasma currents during crescent phase

(t = 1402.29)

Total toroidal current density, ϕ=0

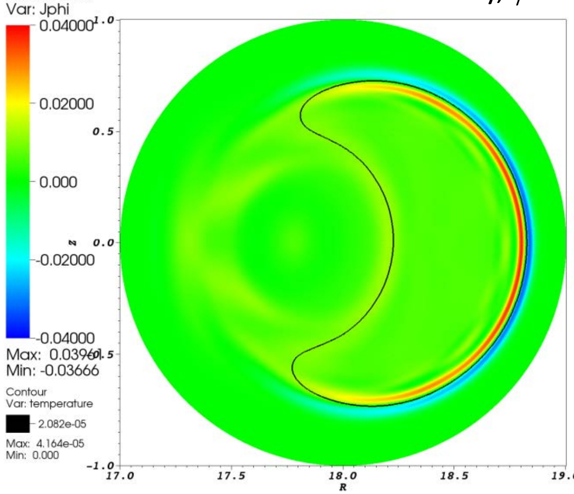

n>0 toroidal current density, ϕ=0

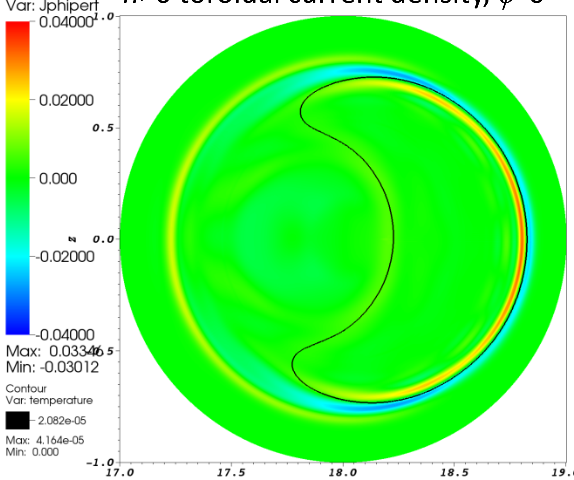

n>0 toroidal current density
on transformed T=2.08×10^{-5} surface

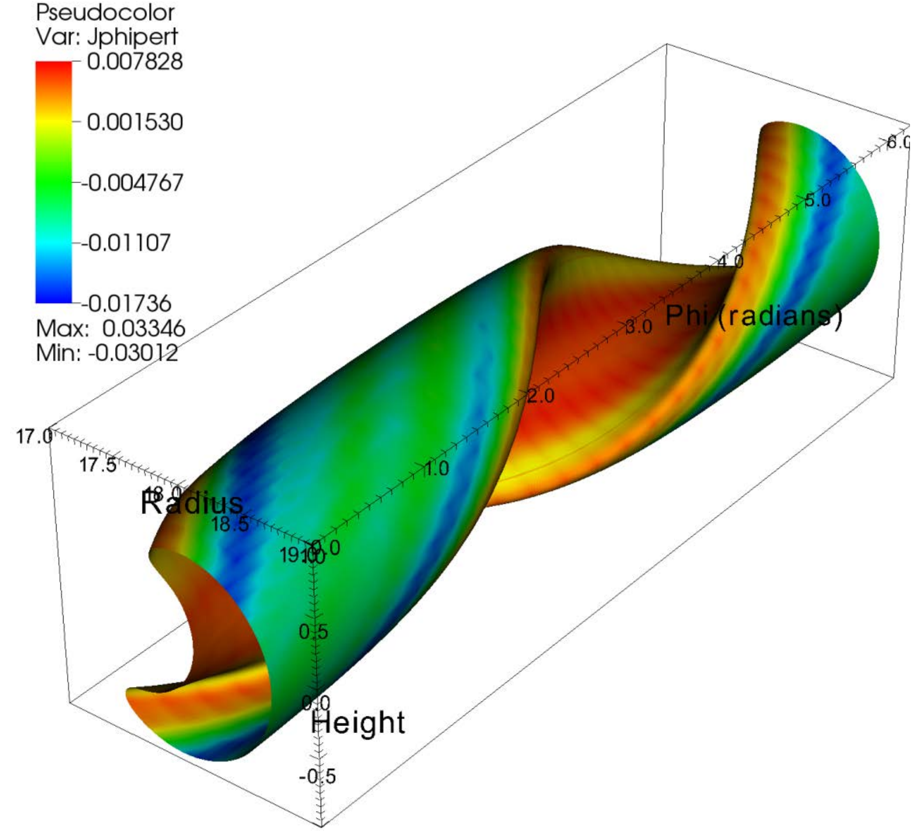

Plasma displacement is stopped by interaction between plasma surface currents and those in the ideal wall.

Increasing aspect ratio to 72 reduces toroidal coupling, but does not change mode behavior

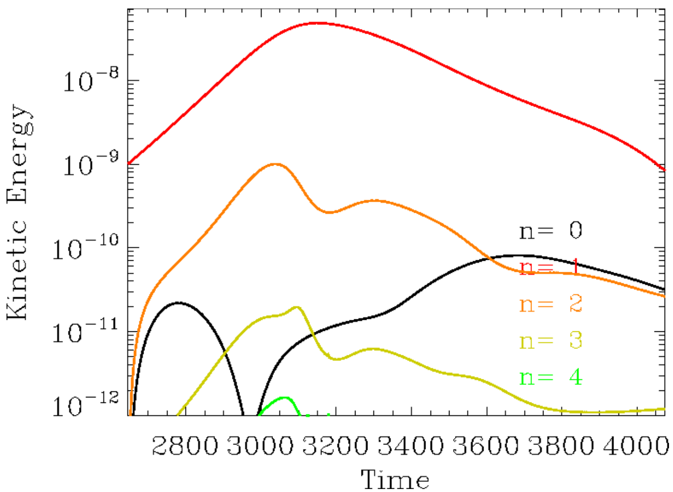

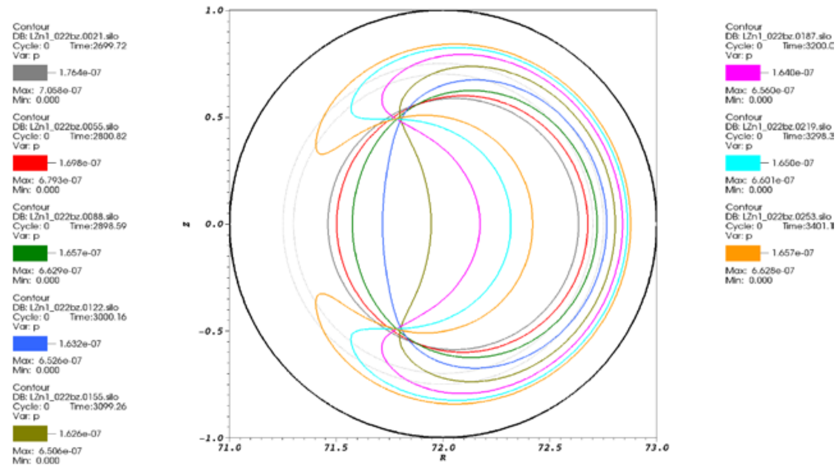

Final state

Resistivity

Vacuum bubble

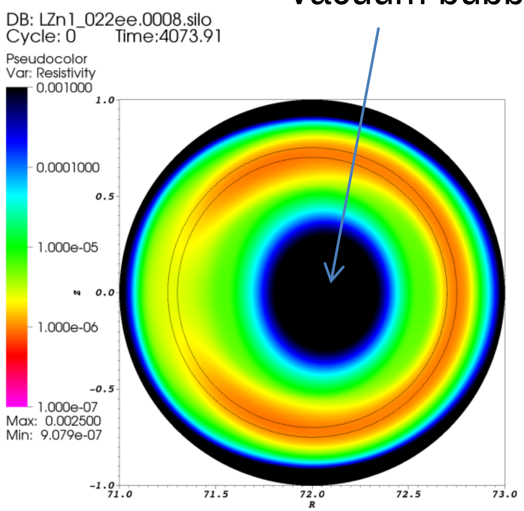

Total toroidal current density, ϕ=0

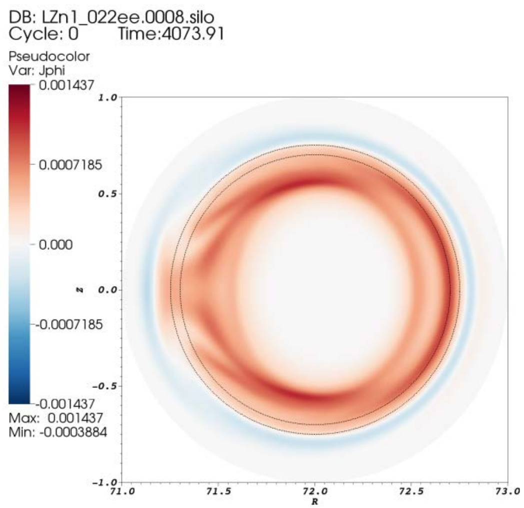

***n*>0 toroidal current density, ϕ=0**

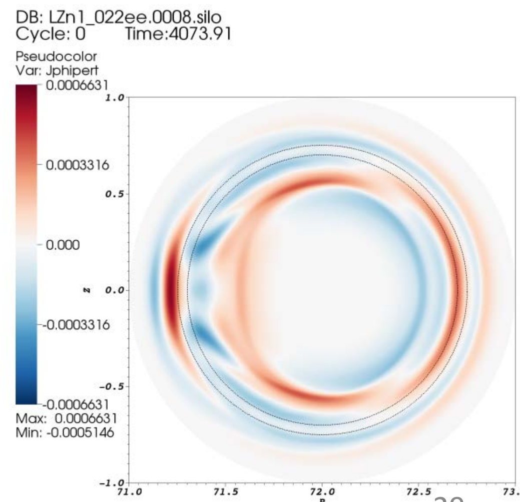

Segmented Tile Model

- Tiles are modeled as an annular region inside the computational domain from r=0.7 to r=0.7+δ.

- When not wetted, tiles behave as ordinary vacuum/plasma ($\eta \propto T^{-3/2}$).

- For wetted region of tile surface (0.7 < r < 0.7+δ **AND** $p > [p_{max} + 3p_{min}]/4$), we set $\eta \equiv \eta_{tile} \leq \eta_{plasma}$.

- Outer boundary of annulus is cold ($T = \varepsilon$ for r > 0.7+δ), chills plasma when in thermal contact.

- No special conditions are imposed on velocity or force balance in tile region.

Full 3D Nonlinear behavior with tile surface at 0.7<r<0.75, only wetted part conducting, outer edge cold, $0 \le n \le 9$ (WTK)

Approx. plasma boundary vs. time

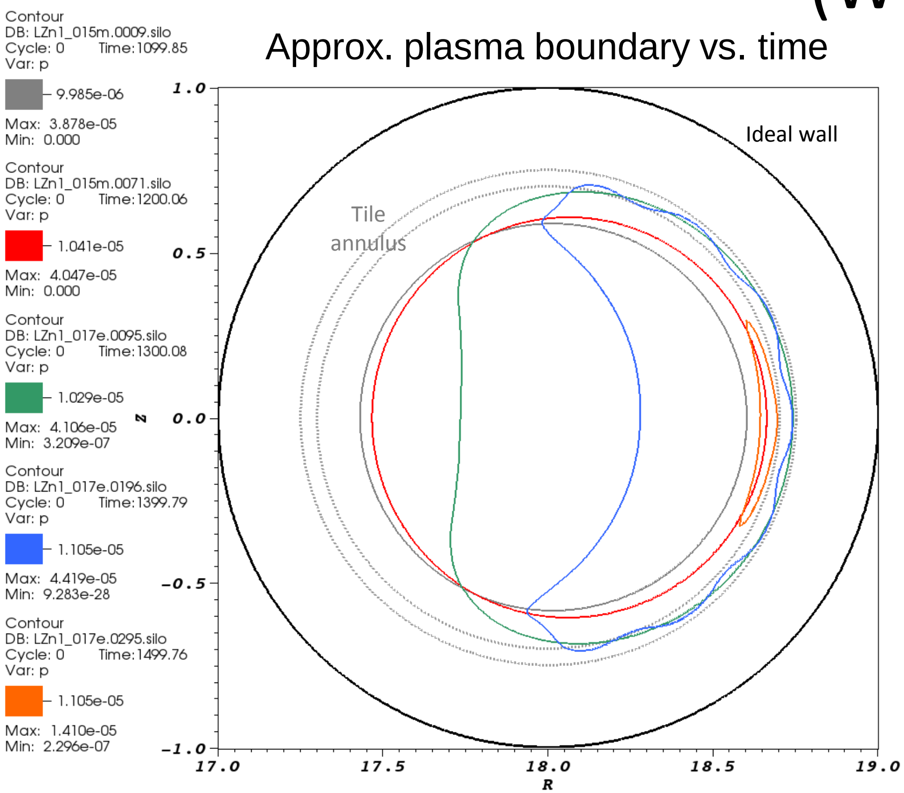

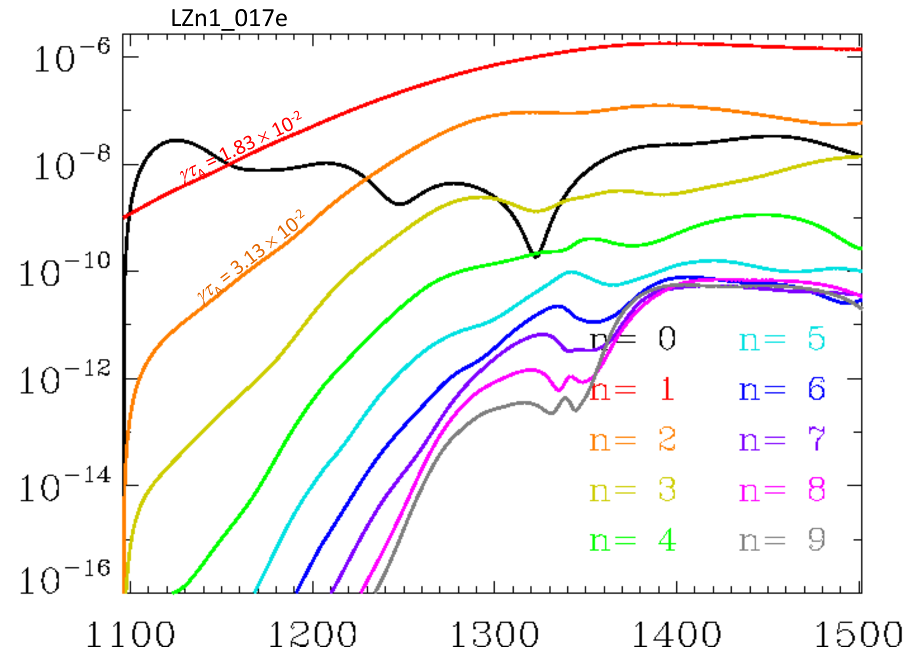

<u>Details</u>:

$\eta_{plas} = 10^{-6}$; $\eta_{vac} \approx 9.5 \times 10^{-4}$; $\eta_{\text{wall}} = 0$; $\eta_{tile} \approx 10^{-7}$

$\mu = 10^{-5}$; $\mu_{\text{H\_tor}} = 10^{-3}$

$\kappa_{\perp} = 10^{-6}$; $\kappa_{||} = 5 \times 10^{2}$

density evolution off

ohmic heating on

Saturates in 300 Alfvén times, develops higher-*m* corrugations, then annihilates on tile surface.

Circle current (before wetting)

(t = 1204.20)

Resistivity

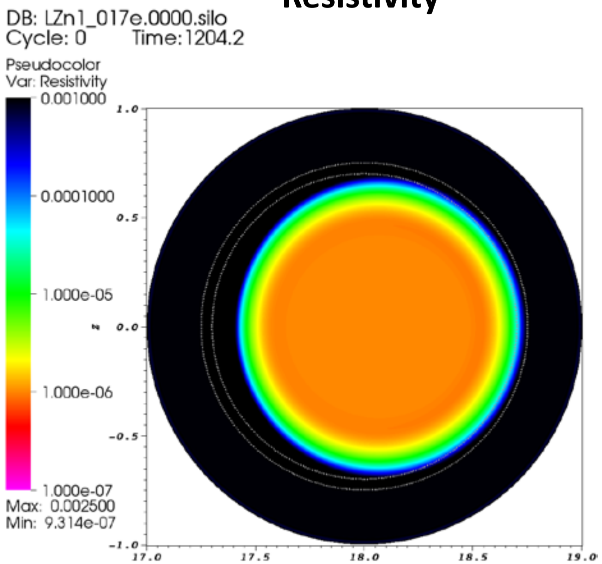

Total toroidal current density, ϕ=0

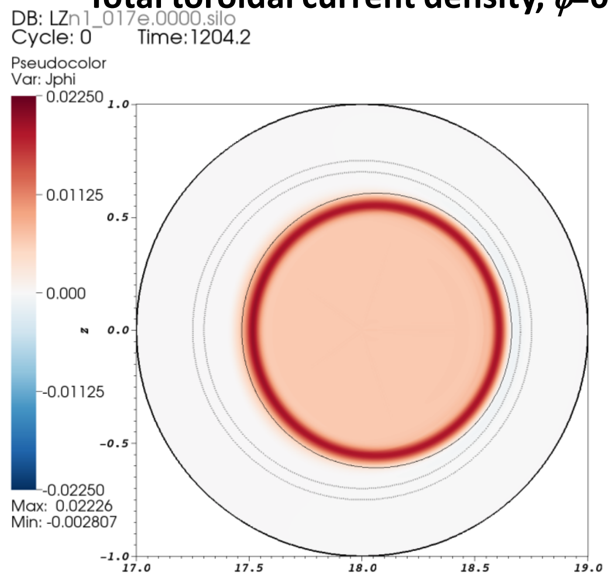

n>0 toroidal current density, ϕ=0

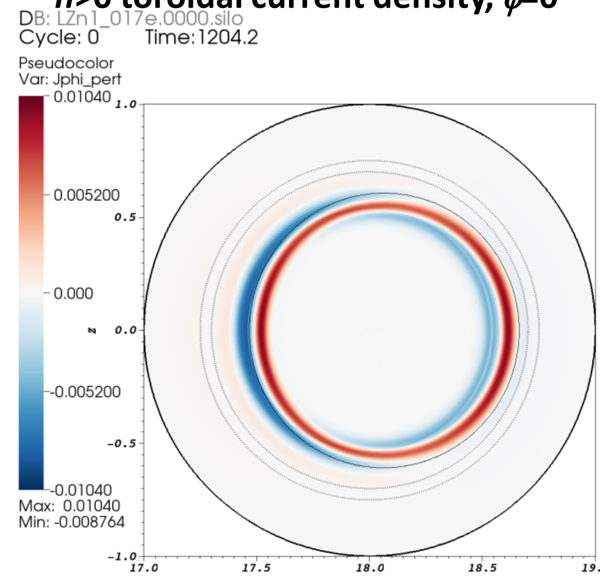

No wetted region

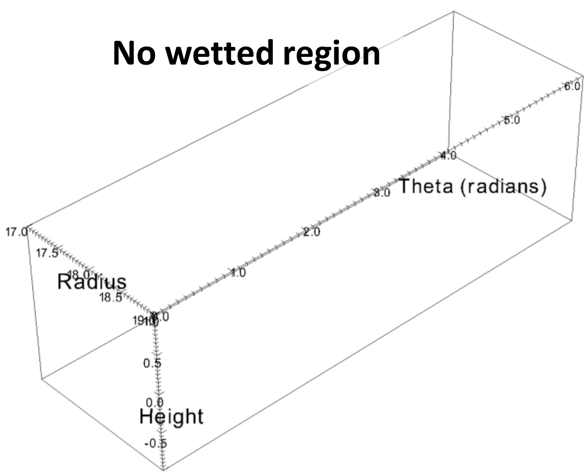

Total toroidal current density, inner tile surface

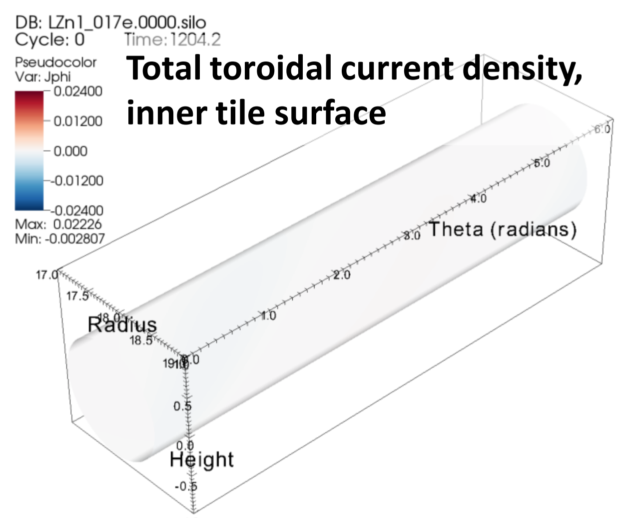

D current

(t = 1300.08)

Resistivity

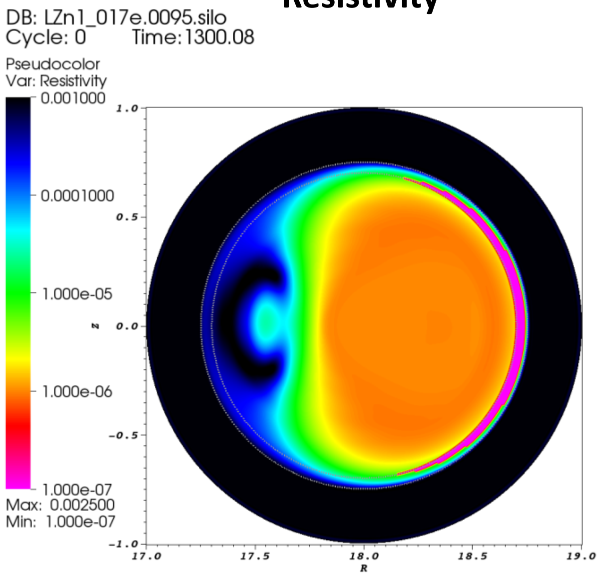

Total toroidal current density, ϕ=0, detail

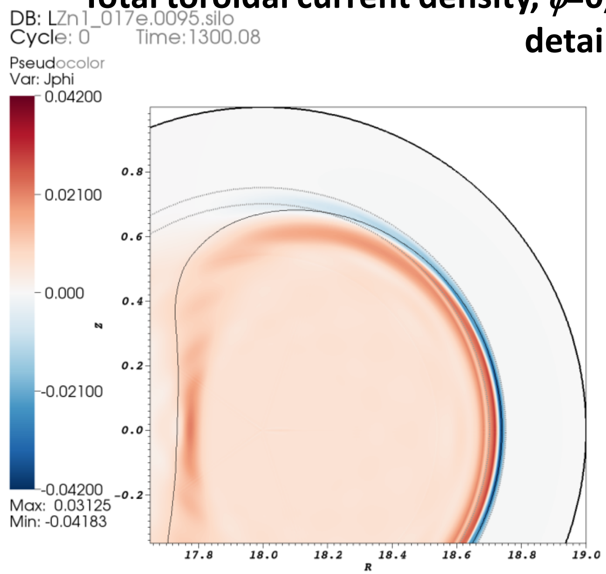

***n*>0 toroidal current density, ϕ=0, detail**

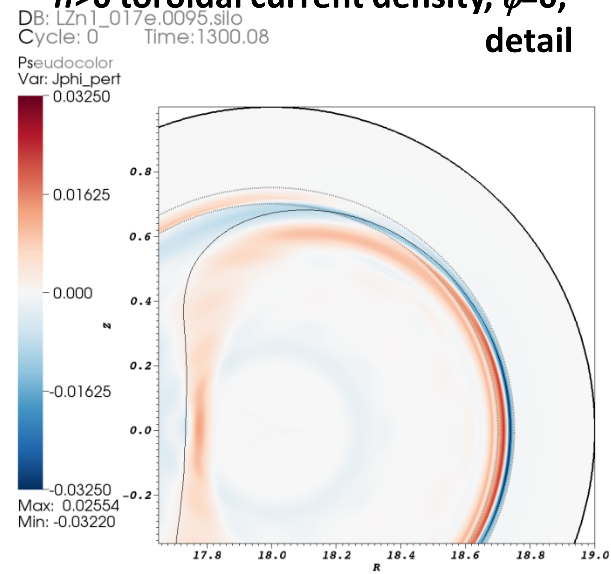

Wetted region

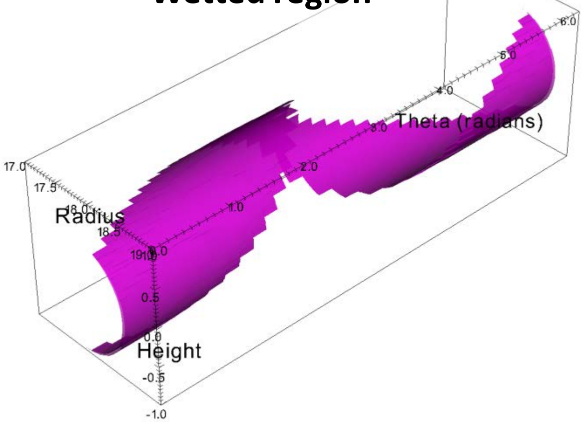

Total toroidal current density, inner tile surface

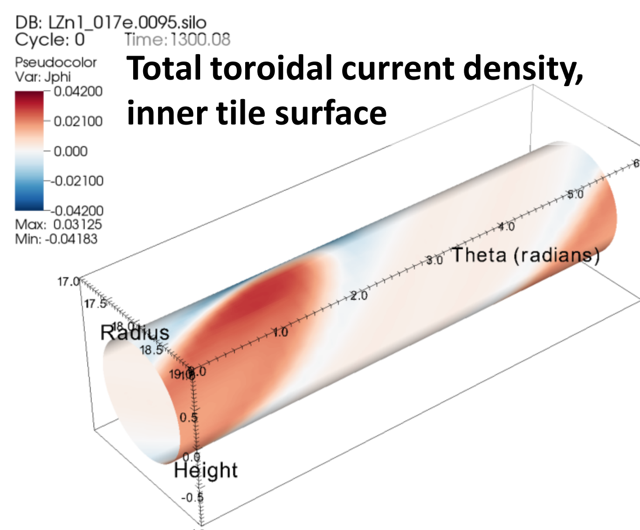

Corrugated crescent current

(t = 1399.79)

Resistivity

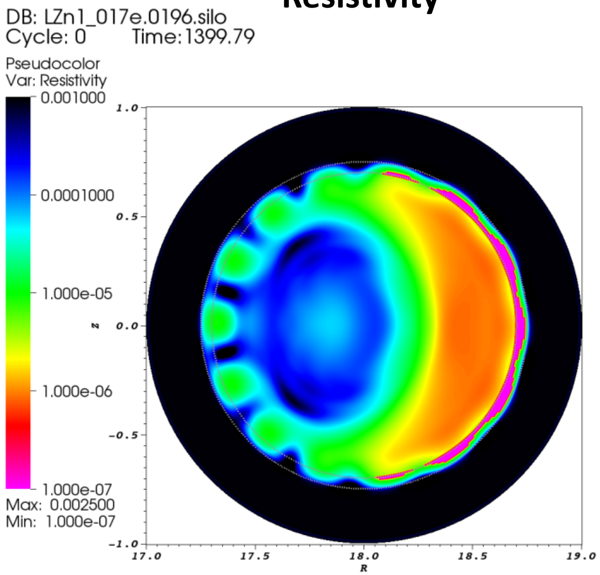

Total toroidal current density, ϕ=0, detail

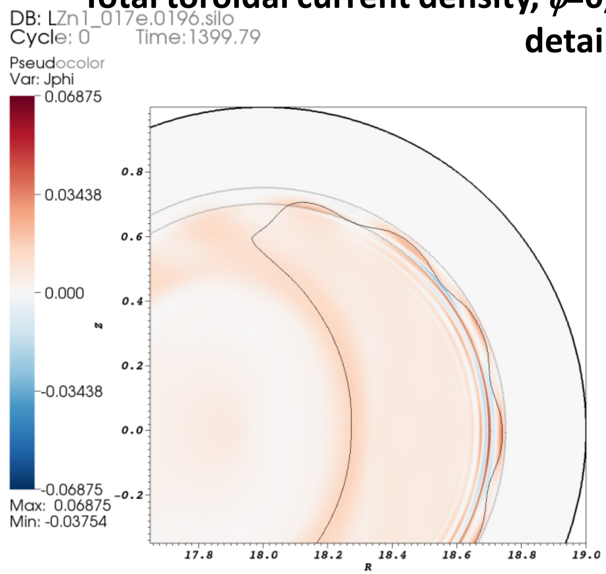

***n*>0 toroidal current density, ϕ=0, detail**

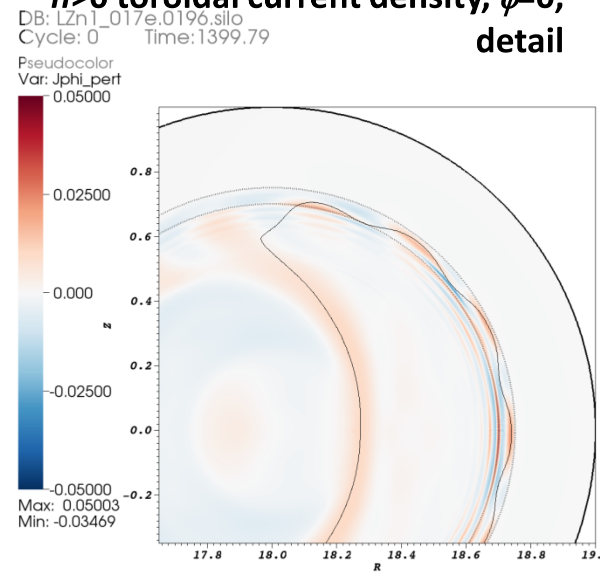

Wetted region

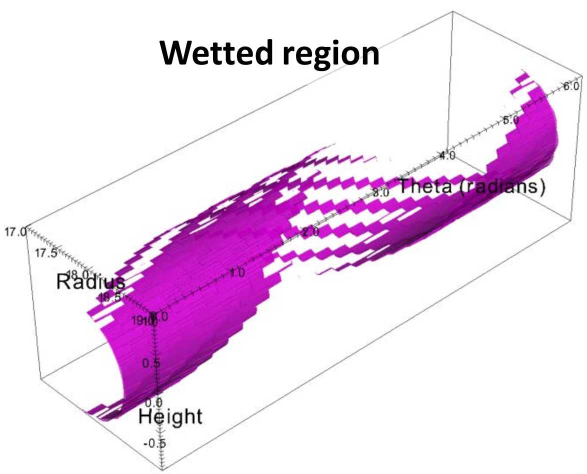

Total toroidal current density, inner tile surface

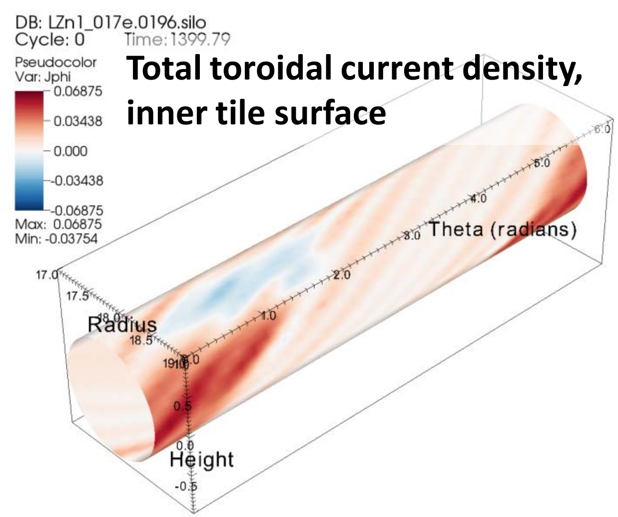

Varying tile resistivity makes little difference

$\eta_{\text{tile}} = 10^{-8}$

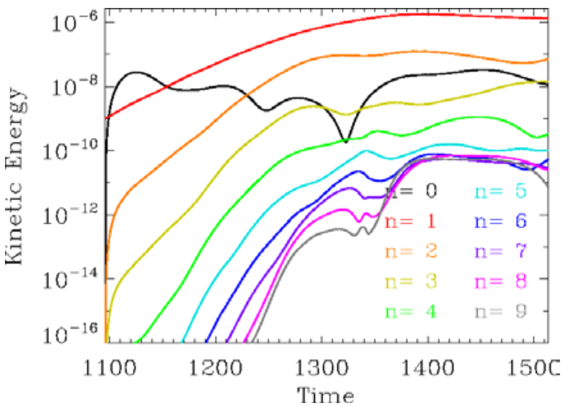

$\eta_{\text{tile}} = 10^{-7}$

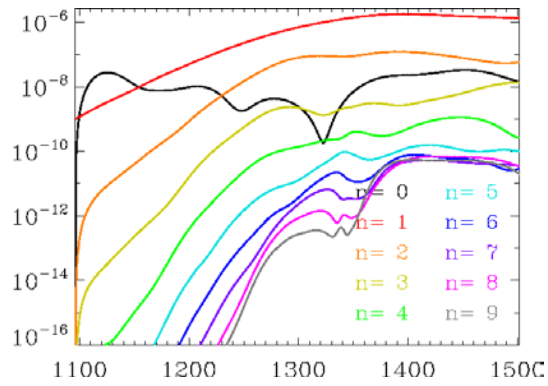

$\eta_{\text{tile}} = 10^{-6}$

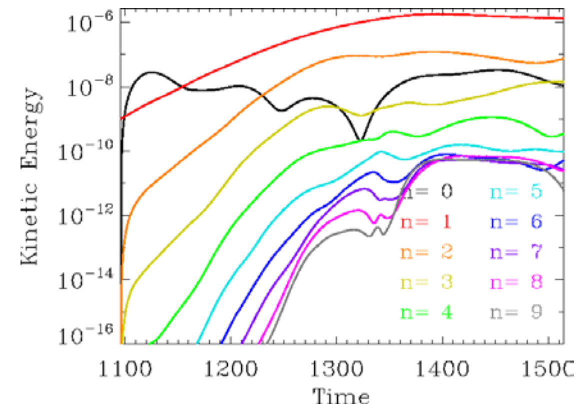

Total toroidal current density, ϕ=0

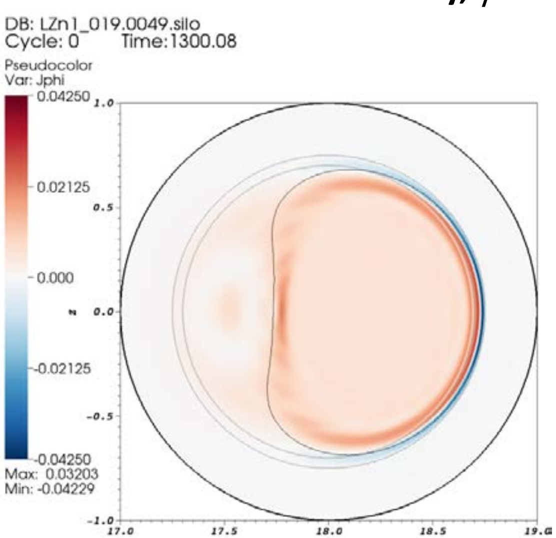

Total toroidal current density, ϕ=0, detail

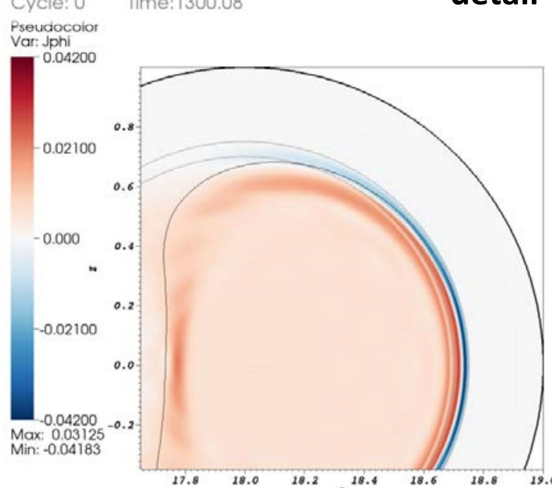

Total toroidal current density, ϕ=0

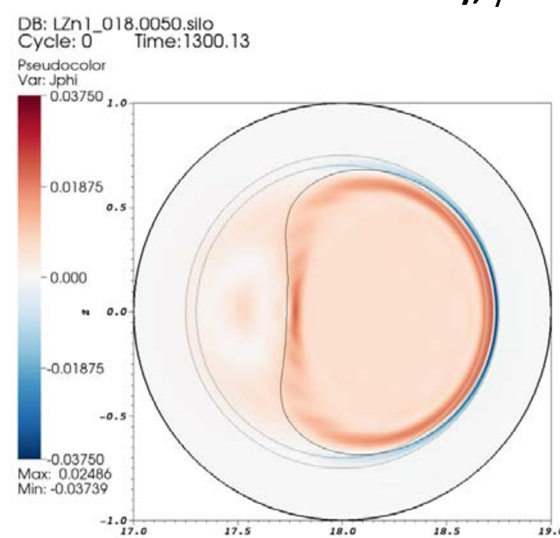

Conclusions

- Although a number of approximations must be made, the M3D code can represent a reasonable facsimile of the ideal straight-cylinder equilibrium with surface current.

- Because it solves the full set of time-dependent resistive MHD equations in three dimensions, M3D sees more complex behavior than the idealized saturated kink solution, namely unstable modes with $n>1$ and the formation of a vacuum bubble. This latter phenomenon, which is physically correct for an equilibrium with no shear*, complicates the comparison.

- The interaction of the plasma surface currents with the ideal wall in the free boundary kink case appears to be in line with the DSC result.

- In the wall-touching kink case, tile currents interact with the plasma surface ("Hiro") current to slow plasma motion, as in the DSC result. As in DSC, the plasma retains finite velocity normal to the tile surface, and can penetrate it on a time scale longer than that of the ideal kink.

*M.N. Rosenbluth, D.A. Monticello, H.R. Strauss, and R.B. White, *Phys. Fluids* **19**, 1987 (1976).

Future Work

- The lack of a vacuum bubble in the DSC result should be understood.

- Still at issue is the effect of the M3D velocity boundary condition on disruption calculations in which the plasma comes into contact with a resistive first wall at the computational boundary.
  - DSC results have not been published for such a scenario.
  - M3D results to date suggest that the effect of this condition on the sharing of plasma current with the wall is minor; current diffuses on the wall resistive time scale regardless of plasma flow.